Nucleophosmin as a Candidate Prognostic Biomarker of Ewing's Sarcoma Revealed by Proteomics

Kazutaka Kikuta,[1,5] Naobumi Tochigi,[2] Tadakazu Shimoda,[2] Hiroki Yabe,[5] Hideo Morioka,[5] Yoshiaki Toyama,[5] Ako Hosono,[3] Yasuo Beppu,[4] Akira Kawai,[4] Setsuo Hirohashi,[1] and Tadashi Kondo[1]

Abstract

Purpose: We aimed to identify novel prognostic biomarkers for Ewing's sarcoma by investigating the global protein expression profile of Ewing's sarcoma patients.

Experimental Design: We examined the proteomic profile of eight biopsy samples from Ewing's sarcoma patients using two-dimensional difference gel electrophoresis. Three patients were alive and continuously disease-free over 3 years after the initial diagnosis (good prognosis group) and five had died of the disease within 2 years of the initial diagnosis (poor prognosis group).

Results: The protein expression profiles produced using two-dimensional difference gel electrophoresis consisted of 2,364 protein spots, among which we identified 66 protein spots whose intensity showed >2-fold difference between the two patient groups. Mass spectrometric protein identification showed that the 66 spots corresponded to 53 distinct gene products. Pathway analysis revealed that 31 of 53 proteins, including nucleophosmin, were significantly related to bone tissue neoplasms ($P < 0.000001$). The prognostic performance of nucleophosmin was evaluated immunohistochemically on an additional 34 Ewing's sarcoma cases. Univariate and multivariate analyses revealed that nucleophosmin expression significantly correlated with overall survival ($P < 0.01$).

Conclusions: These results establish nucleophosmin as a candidate of independent prognostic marker for Ewing's sarcoma patients. Measuring nucleophosmin in biopsy samples before treatment may contribute to the effective management of Ewing's sarcoma.

Ewing's sarcoma is the second most common primary malignant bone tumor in children and adolescents. Despite significant progress regarding intensive chemotherapy protocols and local control measures, 30% to 40% of patients with localized Ewing's sarcoma and 80% of patients with metastatic Ewing's sarcoma at diagnosis die due to disease progression within 5 years (1). More intensified first-line chemotherapy regimens or combinations of chemotherapeutic agents improve clinical outcome compared with conventional chemotherapy (2, 3). However, such therapies may result in serious toxicity, including fatal gastrointestinal toxicity, grade 3 or 4 infections, and severe myelosuppression (4–6). The patients could thus benefit from less aggressive regimens by avoiding the higher risk of toxicity associated with overtreatment. Indeed, approximately two-thirds of patients with localized Ewing's sarcoma are cured with conventional therapy alone (7, 8). Therefore, the identification of prognostic factors may lead to the development of risk-adapted treatment strategies for Ewing's sarcoma.

Clinical factors currently evaluated have limited prognostic value; the presence of metastases at diagnosis, which is the most unfavorable prognostic factor for Ewing's sarcoma, concerns only ~25% of Ewing's sarcoma patients (9). The prognostic value of other clinical and pathologic features that correlated with prognosis of Ewing's sarcoma, including the site and size of the lesion and the age of the patient (1, 10), has decreased following recent advances in treatment (11). For instance, in earlier studies, tumors >8 cm were associated with a worse prognosis (12), whereas tumor size is not assumed as definitive prognostic factor in studies using the more intensive EW92 protocol (13).

In recent years, high-throughput screening technologies such as array-based comparative genomic hybridization analysis and cDNA microarray technology have been used to identify up-regulated or down-regulated genes with prognostic value for Ewing's sarcoma (14–19). These comprehensive studies suggested the presence of a poor prognosis signature at diagnosis and identified several genes that may be involved in the process of invasion and metastasis in Ewing's sarcoma.

Emerging technologies that examine the overall features of the expressed proteins, that is, proteomics, have identified many candidate proteins associated with early diagnosis (20),

Authors' Affiliations: [1]Proteome Bioinformatics Project, National Cancer Center Research Institute; [2]Diagnosis Pathology Division, [3]Pediatric Oncology Division, and [4]Orthopedic Surgery Division, National Cancer Center Hospital; [5]Department of Orthopedic Surgery, Keio University School of Medicine, Tokyo, Japan

Received 7/24/08; revised 12/17/08; accepted 1/10/09; published OnlineFirst 4/7/09.

Grant support: Ministry of Health, Labor and Welfare and Program for Promotion of Fundamental Studies in Health Sciences of the National Institute of Biomedical Innovation of Japan.

The costs of publication of this article were defrayed in part by the payment of page charges. This article must therefore be hereby marked *advertisement* in accordance with 18 U.S.C. Section 1734 solely to indicate this fact.

Note: Supplementary data for this article are available at Clinical Cancer Research Online (http://clincancerres.aacrjournals.org/).

Requests for reprints: Tadashi Kondo, Proteome Bioinformatics Project, National Cancer Center Research Institute, 5-1-1 Tsukiji, Chuo-ku, Tokyo 104-0045, Japan. Phone: 81-3-3542-2511, ext. 3004; Fax: 81-3-357-5298; E-mail: takondo@ncc.go.jp.

doi:10.1158/1078-0432.CCR-08-1913

Translational Relevance

In Ewing's sarcoma, a novel prognostic modality has long been desired to select the patients that would benefit from intensified treatment. We performed a proteomic study using incisionally biopsied samples before treatment. A comparative protein expression study in 8 patients identified nucleophosmin as a novel prognostic biomarker. A subsequent immunohistochemical study on a further 34 cases established the correlation between higher nucleophosmin expression and poor prognosis. In our study, nucleophosmin was identified as a novel candidate prognostic biomarker through the use of modern global protein expression modalities. Our study suggests the possible use of nucleophosmin expression for personalized medicine for Ewing's sarcoma patients.

differential diagnosis (21), prognosis (22, 23), and response to chemotherapy (24) in various diseases but have not been vigorously employed in the study of Ewing's sarcoma.

In this study, we performed a proteomic study using biopsy samples from Ewing's sarcoma patients. We found that nucleophosmin expression significantly correlated with progression of Ewing's sarcoma. Although aberrant expression of nucleophosmin has been implicated in various other malignancies (25–29), this proteomic study shows its aberrant expression and prognostic utility in Ewing's sarcoma.

Materials and Methods

Patients and clinical information. This study included a total of eight frozen incisional biopsy samples taken before treatment at the time of diagnosis from 8 Ewing's sarcoma patients treated between June 1996 and December 2006. These samples were snap-frozen in liquid nitrogen and stored at -80°C until use. The clinical information of the patients is summarized in Table 1. This project was approved by the ethical review board of the National Cancer Center after signed informed consent was obtained from all patients. All cases were reviewed and histopathologically diagnosed by a certified pathologist (N.T. and T.S.). Clinical staging was determined based on diagnostic imaging criteria according to the Musculoskeletal Tumor Society Surgical staging system (30). Primary tumor size was measured at the greatest tumor dimension on radiographic images, including computed tomography scans and magnetic resonance imaging.

From the 8 cases included in the study, 3 patients were alive and continuously disease-free (CDF) in the follow-up period of at least 3 years from diagnosis and 5 patients were dead of disease (DOD) within 2 years from initial diagnosis. All 5 patients in the latter group developed distant metastases within 7 months from initial diagnosis.

A previous report indicated that Ewing's sarcoma patients with early relapse, defined as relapse within 2 years after initial diagnosis, had shorter survival (31). We grouped the Ewing's sarcoma samples into two groups: the samples from patients that were alive and CDF over 3 years post-diagnosis were defined as the good prognosis group (Table 1, samples 1-3). The samples from patients that were DOD within 2 years were defined as the poor prognosis group (Table 1, samples 4-8).

For the nucleophosmin immunohistochemical expression study, we examined 34 tissues paraffin-embedded before treatment from 34 independent cases (Table 2, samples 9-42). These patients were treated between June 1981 and December 2005 at the National Cancer Center and Keio University Hospital. This project was approved by the ethical review boards of the National Cancer Center and Keio University Hospital after signed informed consent was obtained from all patients in this study. The clinical information concerning the cases used in the immunohistochemical study is summarized in Table 2.

Rearrangement analysis. Total RNA from tumors was extracted by the guanidinium thiocyanate method (ISOGEN, Nippon Gene). Samples were ground in a microcentrifuge tube. cDNA was generated using a first-strand cDNA synthesis kit (Pharmacia Biotech). Total RNA (1-5 μg) was transcribed. PCR was carried out in a 100 mL reaction mixture containing 1 to 7 μL cDNA template, 200 mmol/L deoxynucleotide triphosphates, 0.5 mmol/L of each oligonucleotide primer, and 2.5 units Taq polymerase in a 10 mmol/L Tris-HCl (pH 8.8) containing 50 mmol/L KCl and 1.5 mmol/L $MgCl_2$. The oligonucleotide primers used for the PCR were ESBP-1 (EWS specific), ESBP-2 (FLI-1 specific), and primers specific for ERG, E1AF, and ETV1 (32). PCR was done in 35 cycles under the following protocol: denaturation at 94°C for 1 min, annealing at 65°C for 1 min, and elongation at 72°C for 1 min. The amplified products were visualized on 1% agarose gels.

Protein expression profiling. Frozen samples were crushed to powder with a Multi-beads shocker (Yasui Kikai) with liquid nitrogen. The frozen powder was then treated with urea lysis buffer (6 mol/L urea, 2 mol/L thiourea, 3% CHAPS, 1% Triton X-100). After centrifugation at 15,000 rpm for 30 min, the supernatant was recovered and used in the subsequent protein expression studies.

Two-dimensional difference gel electrophoresis was done as described previously (33). In brief, the internal control sample was prepared by mixing a portion of all individual samples. Five micrograms of the internal control sample and of each individual sample were labeled with Cy3 and Cy5, respectively (CyDye DIGE Fluor saturation dye; GE Healthcare Biosciences) according to the manufacturer's instructions. The differently labeled protein samples were mixed and separated by two-dimensional difference gel electrophoresis. The first dimension separation was achieved using IPG DryStrip gels (24 cm

Table 1. Clinicopathologic features of the cases, the frozen samples of which were examined by proteomics

Case no.	Age/sex (y)	Primary site	Size (cm)	Sample source	Stage*	Metastatic site (first development)	Metastasis time after diagnosis (mo)	Follow-up period after diagnosis (mo)	Follow-up status
1	M/19	Thigh	8	Biopsy	L	None	None	88	CDF
2	F/18	Chest wall	4	Biopsy	L	None	None	70	CDF
3	F/9	Parietal Bone	4	Biopsy	L	None	None	46	CDF
4	M/62	Thigh	8	Biopsy	M	Lymph node, Brain	At diagnosis	12	DOD
5	F/28	Humerus	6	Biopsy	L	Lung	7	6	DOD
6	M/32	Thigh	15	Biopsy	M	Lung	At diagnosis	10	DOD
7	M/12	Ilium	11	Biopsy	L	Bone	7	7	DOD

*Stages I and II defined as localized disease (L) and stage III defined as metastatic disease (M).

length, pI range between 4 and 7; GE Healthcare Biosciences). The second dimension separation was achieved by SDS-PAGE on large-format gels (38 cm length, Bio-craft, Itabashi; ref. 33). The gels were scanned using laser scanners (Typhoon Trio; GE Healthcare Biosciences) at appropriate wavelengths (Fig. 1A). For all spots, the intensity of the Cy5 image was normalized by that of the Cy3 image in the identical gel so that gel-to-gel differences were compensated using the Progenesis PG240 software (Nonlinear Dynamics). System reproducibility was verified by comparing the protein profiles obtained from three independent separations of the same sample (Table 1, case 1). Scatter plot analysis revealed that the standardized intensity of >96.6% of the spots ranged within a 2-fold difference (R = 0.9103; Fig. 1B).

Protein identification by mass spectrometry. The proteins corresponding to the spots detected were identified using mass spectrometry according to our previous report (33). In brief, 100 μg Cy5- or Cy3-labeled proteins were separated by two-dimensional PAGE, recovered as gel plugs, and digested with modified trypsin (Promega). The trypsin digests were subjected to liquid chromatography (Paradigm MS4 dual solvent delivery system; Michrom BioResources) and mass spectrometry using a Finnigan LTQ linear ion trap mass spectrometer (Thermo Electron) equipped with a nano-electrospray ion source (AMR, Megro). The Mascot software (version 2.1; Matrix Science) was used to search for the mass of the peptide ion peaks against the SWISS-PROT database (*Homo sapiens*, 12867 sequence in Sprot_47.8 fasta file).

Functional classification of the identified proteins. Functional classification of the identified proteins was carried out according to their classification in Gene Ontology.[6]

Pathway analysis. Pathway analysis of the identified proteins was done using the MetaCore software analysis tool (GeneGo). MetaCore identifies networks based on a manually curated database containing known molecular interactions, functions, and disease interrelationships using proteome data. The pathways were identified by the probability that a random set of proteins with the same size as the input list would give rise to a particular mapping by chance. The identified networks were traced using the Metacore pre-filter tool. The Disease tab tool was used to automatically trace key proteins associated with disease networks stored in Metacore and to list the P value for each disease listed.

Immunohistochemical study. Nucleophosmin expression was examined immunohistochemically on paraffin-embedded tissues. In brief, 4-μm-thick tissue sections were autoclaved in 10 mmol/L citrate buffer (pH 6.0) at 121°C for 30 min and incubated with an antibody against nucleophosmin (sc-53175; Santa Cruz Biotechnology; 1:500 dilution) at room temperature. Immunostaining was done using the Envision Plus detection system (DAKO). Two observers (N.T. and K.K.) evaluated the staining in a blinded fashion for clinical data.

Statistical analysis. Hierarchical clustering was done using the Expressionist software (Genedata).

Statistical computations were done using the StatView version 5.0 statistical package (SAS Institute). Survival time was defined as the period from diagnosis to last follow-up (or death). Survival rate was estimated by the Kaplan-Meier method (34). The relationship between survival and other variables was investigated using the log-rank test for categorical variables and a score test based on the Cox proportional hazards model for continuous variables. A multivariate model was fitted using Cox regression with significant variables at the univariate level (P < 0.01; ref. 35). Following a large-scale cooperative study by the Japanese Musculoskeletal Oncology Group (36), in which age <16 years and tumor size <10 cm were shown to have a significantly worse clinical outcome by univariate survival analysis, we selected these cutoff values for this analysis.

[6] http://www.geneontology.org

Results

We generated and compared the protein expression profiles between three good prognosis and five poor prognosis Ewing's sarcoma cases using two-dimensional difference gel electrophoresis. We detected 2,364 protein spots that appeared in all the images of the Cy3-labeled internal control sample. Among these 2,364 spots, 66 showed significantly (>2-fold ratio of means) different intensity between the two groups. The localization of the 66 spots on the two-dimensional image is shown in Fig. 1C. Using hierarchical clustering, the 66 spots were classified into two major groups, cluster A (7 spots) and cluster B (59 spots; Fig. 2). The intensity of the 7 spots belonging to cluster A was decreased, whereas that of the 59 spots of cluster B was increased in the poor prognosis group.

Mass spectrometric analysis resulted in the identification of 53 distinct gene products (6 proteins in cluster A and 47 proteins in cluster B) corresponding to the 66 protein spots (Fig. 2; Supplementary Table S1).

Although all six proteins in cluster A belonged to different functional categories as classified in Gene Ontology, most of the proteins in cluster B were divided into eight main categories: cytoskeletal/structural protein, transcription/translation, signal transduction, transport, antiapoptosis, response oxidative stress, acute-phase response, and cell proliferation (Fig. 2).

We further explored the biological significance of the altered protein expression pattern in cluster B based on a manually curated database containing known molecular interactions, functions, and disease interrelationships using MetaCore. We found that 31 (65.9%) of 47 proteins were functionally linked with each other and that the identified network of the 31 proteins was significantly related to bone tissue neoplasms (P < 0.000001; Fig. 2).

In the 31 proteins of cluster B, nucleophosmin was included. Although aberrant expression of nucleophosmin has been implicated in various other malignancies (25–29), its association with Ewing's sarcoma has not been reported previously. Therefore, we validated the correlation of nucleophosmin with prognosis using immunohistochemistry in an additional 34 Ewing's sarcoma cases. Two patterns of nucleophosmin-positive staining were observed, both nuclear: a dot-like pattern and a diffuse-like pattern (Fig. 3). Similar to previous reports (25, 37), cases with nuclear staining for nucleophosmin were considered as nucleophosmin positive (23 of 34 cases; Table 2), whereas cases without staining for nucleophosmin were considered as nucleophosmin negative.

In the follow-up period (median, 57.5 months; range, 8-179 months), 13 of 34 patients were alive and CDF and 21 patients were DOD (Fig. 4A).

The group of nucleophosmin-positive cases included a significantly higher number of DOD patients compared with the nucleophosmin-negative group (P < 0.01, log-rank test; Fig. 4B), showing that nucleophosmin expression correlates with prognosis.

Following univariate analysis, nucleophosmin positivity (P < 0.01) and clinical stage (presence of metastatic disease at diagnosis; P < 0.01) significantly correlated with shorter overall survival. No other factors examined, including the tumor size, age at diagnosis, sex, chemotherapy regimens, tumor resectibility, and primary site, were associated with overall survival (Table 3).

Table 2. Clinicopathologic features of the 34 Ewing's sarcoma cases examined immunohistochemically

Case no.	Sex/age (y)	Primary site	Size (cm)	Sample source	Stage*	Metastatic site (first development)	Metastasis time after diagnosis (mo)	Follow-up period after diagnosis (mo)
9	M/9	Fibula	9	Biopsy	L	None	None	93
10	M/14	Clavicle	15	Biopsy	L	None	None	177
11	M/49	Femur	11	Biopsy	L	None	None	141
12	M/16	Arm	3	Biopsy	L	None	None	93
13	M/25	Rib	5.5	Biopsy	L	None	None	75
14	M/9	Talus	2	Biopsy	L	None	None	70
15	M/1	Tibia	—†	Biopsy	L	None	None	179
16	F/36	Femur	—†	Biopsy	L	None	None	174
17	M/13	Tibia	—†	Biopsy	L	None	None	166
18	F/22	Fibula	6	Biopsy	L	None	None	108
19	M/18	Rib	6.5	Biopsy	L	None	None	105
20	M/35	Thigh	8	Biopsy	L	None	None	126
21	F/36	Arm	4	Biopsy	L	None	None	101
22	M/15	Thigh	16	Biopsy	L	Lung	8	11
23	M/17	Rib	10	Biopsy	L	Multiple bone	7	8
24	M/18	Back	25	Biopsy	L	Lung	6	8
25	M/22	Femur	10	Biopsy	L	Bone	2	14
26	M/37	Ilium	25	Biopsy	M	Lung	At diagnosis	22
27	F/24	Sacrum	10	Biopsy	L	Bone	3	22
28	M/11	Femur	10	Biopsy	L	Bone, brain, lung	1	32
29	F/22	Humerus	18	Biopsy	L	Bone	19	32
30	F/20	Femur	5	Biopsy	L	Lung	41	75
31	M/21	Parietal bone	5	Biopsy	L	Lung	69	94
32	F/19	Humerus	7	Biopsy	L	Lung, bone	43	121
33	M/17	Vertebra	10	Biopsy	L	Lung	12	45
34	F/16	Tibia	20	Biopsy	M	Lung	At diagnosis	16
35	M/18	Fibula	7	Biopsy	L	Bone, lung	9	21
36	M/23	Pelvis	13	Biopsy	M	Lung	At diagnosis	17
37	M/29	Thigh	16	Biopsy	M	Chest	At diagnosis	12
38	F/63	Paravertebra	17	Biopsy	L	None	None	71
39	F/20	Lower leg	10	Biopsy	L	Lung, lymph node	9	14
40	F/56	Forearm	5	Biopsy	M	Lung	At diagnosis	11
41	M/7	Paravertebra	4	Biopsy	L	Brain	15	16
42	F/11	Paravertebra	6	Biopsy	L	Lung	17	22

NOTE: Chemotherapy agents: VACD, vincristine (VCR), actinomycin D (ACT), cyclophosphamide (CYC), and doxorubicin (DOX); IE, ifosfamide (IFO) and etoposide (ETO); THP, therarubicin; CDDP, cisplatin; BLM, bleomycin; MTX, methotrexate; DTIC, dacarbazine. NT, not tested.
*Stages I and II defined as localized disease (L) and stage III defined as metastatic disease (M).
†Tumor size cannot be evaluated.

We investigated whether nucleophosmin expression significantly correlated with the original tumor site and the tumor respectability status. Of the 34 cases in this study, 21 originated at an extra-axial and 13 at an axial site. Nucleophosmin expression did not correlate with the original tumor site (P = 0.87, Fisher's test). Of the 21 extra-axial tumors, 14 were nucleophosmin positive, and nucleophosmin expression correlated with poor prognosis ($P < 0.05$, log-rank test). Of the 13 axial tumors, 9 were nucleophosmin negative; again, nucleophosmin expression significantly correlated with poor prognosis ($P < 0.01$, log-rank test). Therefore, nucleophosmin expression correlated with poor prognosis independent of the original tumor site.

There was no significant difference regarding the prognosis between the resectable (26 of 34) and nonresectable cases (P = 0.1219, log-rank test). Among the resectable tumors, 16 were nucleophosmin positive and had worse prognosis than the remaining 10 nucleophosmin-negative tumors ($P < 0.01$, log-rank test).

Multivariate analysis done on nucleophosmin staining and clinical stage, identified as significant prognostic factors by univariate analysis, revealed that both significantly correlated, as separate variables, with overall survival (P = 0.0063; relative risk, 7.768; 95% confidence interval, 1.783-33.841 and P = 0.0039; relative risk, 5.964; 95% confidence interval, 1.773-20.060, respectively; Table 3).

On a second univariate analysis, we found that nucleophosmin positivity was also a strong negative predictor of overall survival in the 29 of 34 patients that had localized disease at diagnosis ($P < 0.01$; log-rank test; Fig. 4C).

Table 2. Clinicopathologic features of the 34 Ewing's sarcoma cases examined immunohistochemically (Cont'd)

Follow-up status	Nucleophosmin positivity	Fusion gene	Chemotherapy	Chemotherapy agents	Operation	Radiation
CDF	-	NT	VCD + I-based regimens	VCR, CYC, DOX, IFO, etc	Amputation	-
CDF	-	NT	VAIA	VCR, ACT, IFO, DOX	Wide resection	+
CDF	-	NT	VAIA	VCR, ACT, IFO, DOX	Wide resection	-
CDF	-	NT	VCD + I-based regimens	VCR, CYC, DOX, IFO, etc	Wide resection	-
CDF	-	NT	VCD + I-based regimens	VCR, CYC, DOX, IFO, etc	Wide resection	-
CDF	+	NT	VCD + I-based regimens	VCR, CYC, DOX, IFO, etc	-	+
CDF	+	NT	VAC	VCR, ACT, CYC	Amputation	+
CDF	-	NT	VACA	VCR, ACT, CYC, DOX	Amputation	+
CDF	-	EWS/ERG	CYVADIC	CYC, VCR, DOX, DTIC	Wide resection	+
CDF	-	EWS/FLI1 type 2	KS-1	ETO, CDDP, THP, IFO	Wide resection	-
CDF	-	EWS/FLI1 EWSex10/FLI-1ex6	KS-1	ETO, CDDP, THP, IFO	Wide resection	+
CDF	+	NT	KS-1	ETO, CDDP, THP, IFO	Wide resection	-
CDF	+	Not detected	KS-1	ETO, CDDP, THP, IFO	Wide resection	-
DOD	+	NT	National Cancer Institute protocol (VAC + IE)	VCR, DOX,CYC + IFO, ETO	Wide resection	+
DOD	+	EWS R1 rearrangement	ACT + CDDP	ACT, CDDP	-	+
DOD	+	NT	VACA	VCR, ACT, CYC, DOX	Intralesional resection	+
DOD	+	NT	VAIA	VCR, ACT, IFO, DOX	-	-
DOD	-	NT	National Cancer Institute protocol (VAC + IE)	VCR, DOX,CYC + IFO, ETO	-	+
DOD	+	NT	National Cancer Institute protocol (VAC + IE)	VCR, DOX,CYC + IFO, ETO	-	+
DOD	+	NT	VAC	VCR, ACT, CYC	Amputation	+
DOD	+	NT	VAIA	VCR, ACT, IFO, DOX	Wide resection	+
DOD	+	NT	T11	CYC, DOX,MTX, VCR + BLM, CYC, ACT + CYC, DOX, MTX	Wide resection	-
DOD	+	NT	National Cancer Institute protocol (VAC + IE)	VCR, DOX,CYC + IFO, ETO	-	+
DOD	+	NT	T11	CYC, DOX,MTX, VCR + BLM, CYC, ACT + CYC, DOX, MTX	-	+
DOD	+	NT	T11	CYC, DOX,MTX, VCR + BLM, CYC, ACT + CYC, DOX, MTX	Marginal resection	+
DOD	+	EWS/FLI1 type 2	KS-1	ETO, CDDP, THP, IFO	Wide resection	-
DOD	+	EWS/FLI1 type 1	KS-1	ETO, CDDP, THP, IFO	Wide resection	+
DOD	+	NT	KS-1	ETO, CDDP, THP, IFO	-	+
DOD	+	EWS/FLI1 type 2	KS-1	ETO, CDDP, THP, IFO	Intralesional resection	+
DOD	+	NT	KS-1	ETO, CDDP, THP, IFO	Intralesional resection	+
DOD	-	EWS/FLI1 type 1	KS-1	ETO, CDDP, THP, IFO	Marginal resection	+
DOD	+	NT	KS-1	ETO, CDDP, THP, IFO	Wide resection	-
DOD	+	Not detected	KS-1	ETO, CDDP, THP, IFO	Marginal resection	-
DOD	+	EWS/FLI1 type 1	KS-1	ETO, CDDP, THP, IFO	Intralesional resection	+

Discussion

The identification of novel prognostic biomarkers for Ewing's sarcoma is required to improve the management of Ewing's sarcoma. Global genomic and transcriptomic expression studies conducted to identify prognostic biomarkers for Ewing's sarcoma resulted in the identification of *MTA1*, *CDH11* (14), *STEAP1*, *NKX2-2*, and *CCND1* (15), gains in chromosomes 1q, 8, and 12 and deletions of 1p as genetic lesions implicated in the progression of Ewing's sarcoma (16–18). Although these comprehensive studies may have the potential to further increase our understanding of the biology of Ewing's sarcoma and to lead to the development of practical tumor markers to support individualized therapy, practical prognostic biomarkers of Ewing's sarcoma are presently not used in a clinical setting.

Proteomic studies have unique advantages on other omics studies. The proteome is a functional translation of the genome, directly regulating cell phenotypes, and is thus a rich source of biomarkers. With this notion, we have established the gel-based proteomics system for cancer research and applied it to the Ewing's sarcoma proteomic study presented here. This is the first report using a proteomic approach to develop prognostic biomarkers for Ewing's sarcoma.

We identified 6 down-regulated and 47 up-regulated proteins in Ewing's sarcoma cases with poor prognosis. Functional classification revealed that these identified proteins belonged to a variety of functional pathways, including cytoskeletal/structural organization, transcription/translation, signal transduction, transport, antiapoptosis, response-oxidative stress, acute-phase response, and cell proliferation. The results of functional classification may suggest that the proteomic alterations observed may be a part of global series of functionally interconnected molecular lesions that include transcriptional and translational aberrations, which, taken together, include both the causes and the results of carcinogenesis and cancer progression.

This proteome study identified or confirmed the presence of several molecular aberrations concerning Ewing's sarcoma. The

47 proteins found to be up-regulated included neuron-specific enolase, which has been found to be associated with poor prognosis in Ewing's sarcoma (38, 39).

Nucleophosmin was included in the 47 proteins found to be up-regulated. Nucleophosmin overexpression has been related to carcinogenesis and tumor progression in prostate (25), gastric (26), colon (27), ovarian (28), and urinary bladder carcinomas (29). However, the association of nucleophosmin with Ewing's sarcoma has not been reported previously, including, importantly, in previous genomic and transcriptomic studies of Ewing's sarcoma (14–19). This may be due to discordance between mRNA and protein expression, the fact

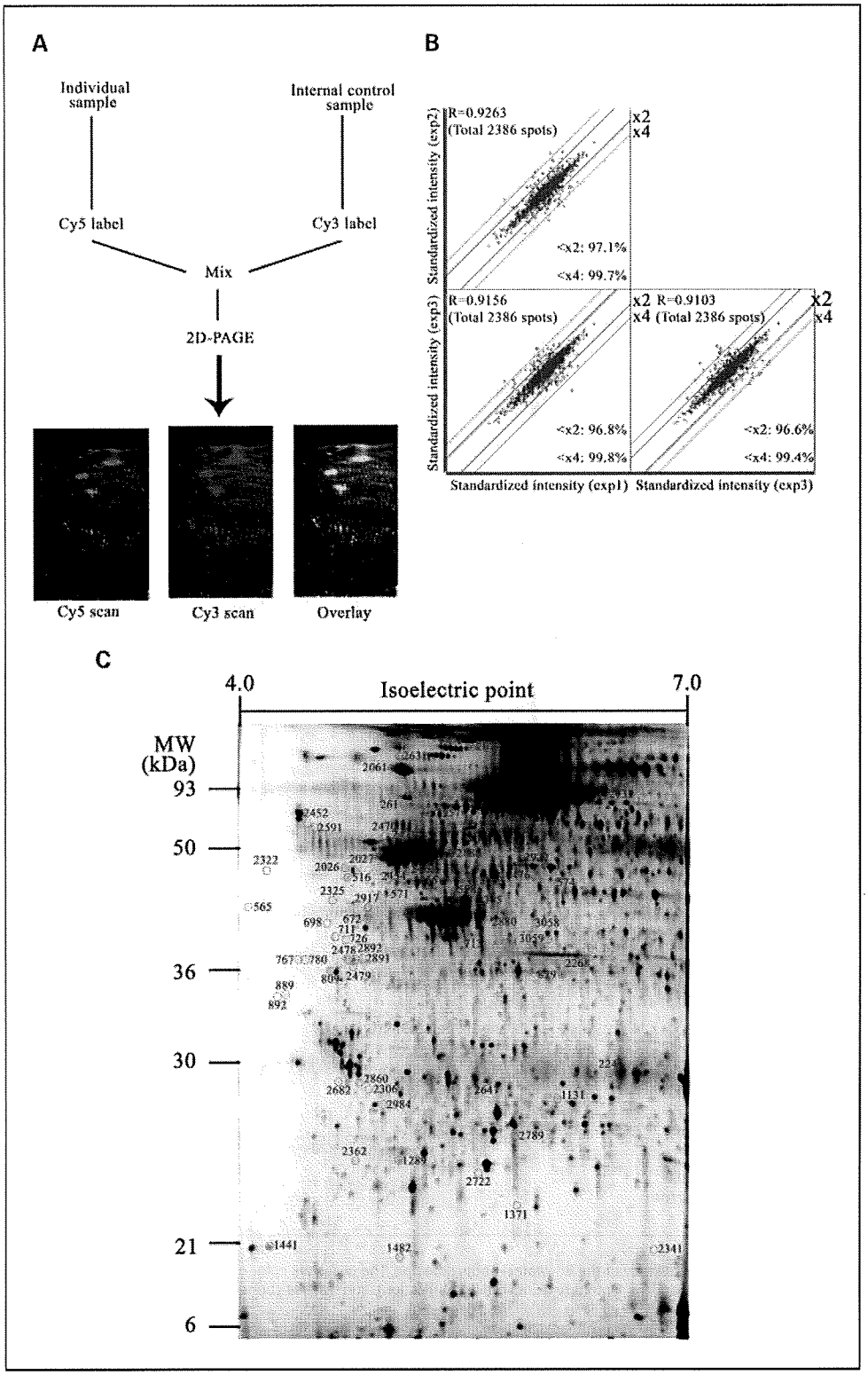

Fig. 1. Identification of proteins differentially expressed in Ewing's sarcoma. *A*, schematic workflow of sample preparation for quantitative analysis. Protein lysates are labeled with fluorescent dyes of different wavelengths of excitation and emission. Cy3-labeled samples are simultaneously mixed and divided into Cy5-labeled samples. Then, mixture of Cy3- and Cy5-labeled lysates are coseparated by two-dimensional difference gel electrophoresis. The gel is scanned with two wavelengths, each specific either for Cy3 or Cy5 dye. *B*, scattergram of expression profile of Ewing's sarcoma tissues. Comparison of data from three independent experiments revealed the high reproducibility of protein expression profiling. *C*, representative two-dimensional image of proteins detected in Ewing's sarcoma tissues. The 66 spots identified in this study are circled and numbered. The spot numbers correspond to those in Fig. 2 and Supplementary Table S1.

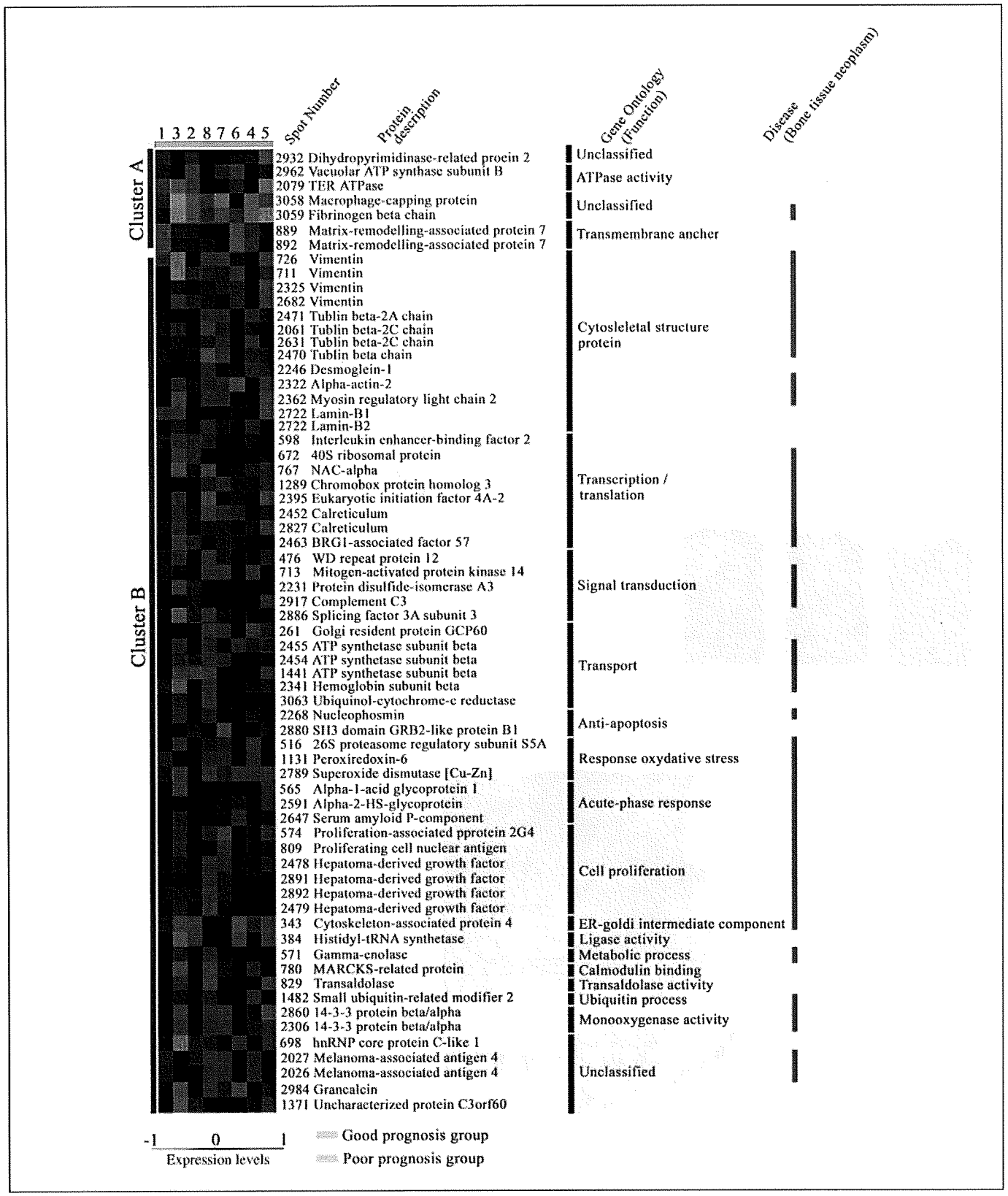

Fig. 2. Hierarchical clustering of the 8 Ewing's sarcoma cases based on the intensity of the 66 protein spots detected. The cases are color-coded as yellow (good prognosis group) or light blue (poor prognosis group). The spot numbers, protein names, Gene Ontology (functional classification), and disease (bone tissue neoplasms; color-coded as red) related proteins are shown (*right*).

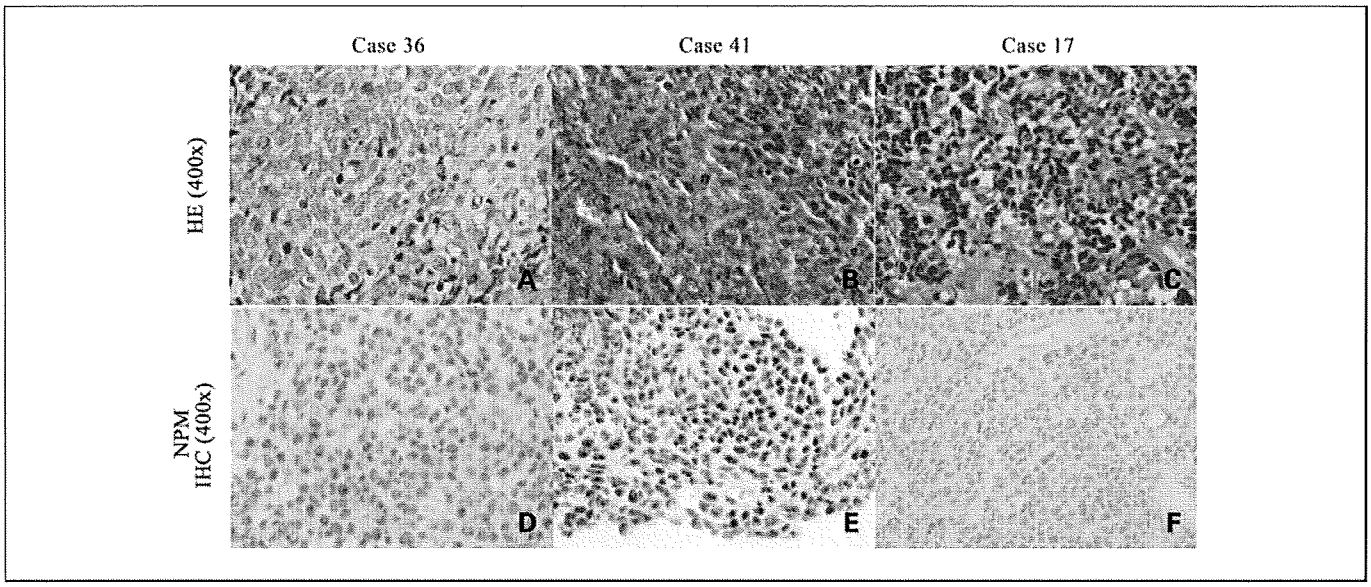

Fig. 3. Nucleophosmin expression was observed in Ewing's sarcoma by immunohistochemistry. *A* to *C*, H&E staining of Ewing's sarcoma cases. Strongly stained nucleophosmin nuclear expression was observed in tumor cells. *D*, dot-like pattern staining. *E*, diffuse-like pattern staining. *F*, not observed stained nucleophosmin nuclear expression. Case numbers correspond to those in Table 2. Magnification, ×400.

that a different patient population was studied, or, finally, the fact that transcriptome and proteome studies cannot uncover entire genome data. These results, therefore, also suggest that studies using proteomic tools are able to reveal unique molecular aspects of Ewing's sarcoma.

Network analysis showed that nucleophosmin is linked with four proteins (c-myc, nuclear factor-κB, Sp1 and p53), which have also been found to be implicated in poor prognosis in Ewing's sarcoma (Supplementary Fig. S1). c-myc has been identified as a potential EWS-ets target gene (40) and as promoting malignant progression of Ewing's sarcoma (41). Activation of nuclear factor-κB was found to contribute to resistance of Ewing's sarcoma cells to apoptosis (42). Coexpression of Sp1 with EWS-ets oncoprotein enhances activation of vascular endothelial growth factor, the expression of which was shown to be a negative predictor of survival in Ewing's sarcoma (43). Aberrations in p53 were found in ~10% of Ewing's sarcoma cases and were associated with shorter survival (44, 45). Taken together, these observations suggest that nucleophosmin can be a single biomarker probably by linking these functionally different proteins. Ewing's sarcoma is characterized by a translocation between the *EWS* gene and a member of the *ETS* family of transcriptional factors (46). The EWS/ETS fusion protein has an altered transcriptional activity and modulates the expression of several downstream target genes (47, 48). The association between the EWS/ETS fusion protein and nucleophosmin should be further investigated.

Nucleophosmin may be used as a novel prognostic biomarker of patients with Ewing's sarcoma. We found that nucleophosmin expression correlated with clinical outcome in 34 Ewing's sarcoma patients. Univariate and multivariate analyses revealed that nucleophosmin expression along with clinical stage (presence of metastases at diagnosis) was an independent prognostic factor in Ewing's sarcoma patients. Furthermore, nucleophosmin expression was also a significant

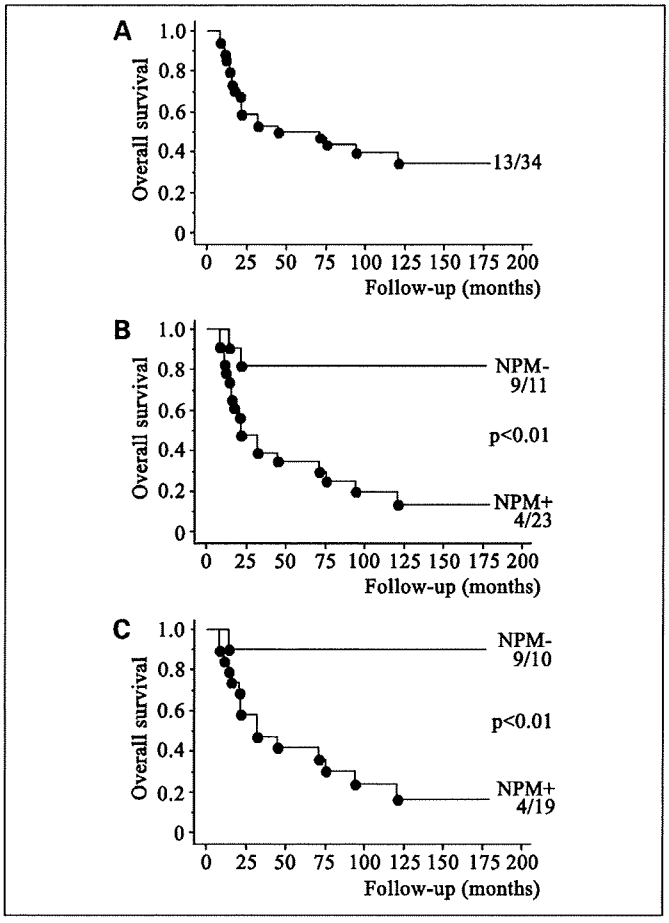

Fig. 4. Kaplan-Meier estimated overall survival curves are illustrated for all patients ($n = 34$; *A*), for all patients based on nucleophosmin positivity (*B*), and for patients with localized disease ($n = 29$) by nucleophosmin positivity (*C*). Statistically significant differences in overall survival periods were observed between the nucleophosmin-positive and nucleophosmin-negative cases both for all cases ($P < 0.01$, log-rank test) and the cases with localized disease ($P < 0.01$, log-rank test).

Table 3. Univariate and multivariate analyses of prognostic factors

Variable	Univariate survival analysis				Multivariate survival analysis	
	No. cases	No. alive	Univariate *P*	Risk ratio (95% confidence interval)	*P*	Relative risk (95% confidence interval)
Age at diagnosis (y)						
<16	9	5	0.3209	1		
≥16	25	8		1.738 (0.583-5.180)		
Sex						
M	22	10	0.5325	1		
F	12	3		0.517 (0.207-1.288)		
Primary site						
Extremity	21	10	0.212	1		
Axial	13	3		1.736 (0.730-4.126)		
Tumor size (cm)*						
<10	16	7	0.0182	1		
≥10	15	2		2.952 (1.202-7.251)		
Clinical stage						
Localized	29	13	<0.01	1	0.0039	1
Metastatic	5	0		5.238 (1.697-16.164)		5.964 (1.773-20.060)
Chemotherapy regimens						
Including IE	17	4	0.0629	1		
Not including IE	17	9		0.425 (0.955-5.791)		
Tumor resectibility						
Resectable	26	12	0.1219	1		
Nonresectable	8	1		2.004 (0.200-1.244)		
Nucleophosmin immunohistochemistry						
Negative	11	9	<0.01	1	0.0063	1
Positive	23	4		7.425 (1.715-32.147)		7.768 (1.783-33.841)

*Tumor size could not be evaluated in 3 Ewing's sarcoma cases.

prognostic factor in patients with localized disease. Applying these findings in a clinical setting poses the next challenge. As the incisional biopsy is a procedure done routinely in establishing the diagnosis in Ewing's sarcoma, the immunohistochemical examination of nucleophosmin expression can be done without any additional invasive examinations.

Although previous reports have suggested a possible association between nucleophosmin and malignancies, the functional role of nucleophosmin in Ewing's sarcoma is still unclear. Nucleophosmin overexpression has been reported to be involved in human tumorigenesis (49, 50). In one study, it led to increased proliferation and inhibition of apoptosis in tumor cells; overexpression of nucleophosmin reduced the percentage of cells in the G_1 phase and increased the S-phase population in the p53-negative cells but induced cell cycle arrest in normal cells. Conducting further basic research on the function of nucleophosmin will pave the way for further understanding of the molecular background of Ewing's sarcoma and, hopefully, for novel diagnostic and therapeutic applications.

In conclusion, global protein expression profiling revealed the proteomic background of Ewing's sarcoma and identified novel associations of several proteins with progression of Ewing's sarcoma. Of the proteins with expression that may have prognostic value, we successfully validated the association of nucleophosmin expression with poor prognosis. The expression of the other proteins may still have prognostic value and further validation studies may prove it. Evaluation of nucleophosmin expression may allow the identification of poor prognosis Ewing's sarcoma patients who may benefit from highly effective treatment in the future.

Disclosure of Potential Conflicts of Interest

No potential conflicts of interest were disclosed.

Acknowledgments

We thank Chizu Kina and Sachiko Miura for excellent technical support in the immunohistochemical study and Yukiko Fujie for excellent technical support in electrophoresis.

References

1. Cotterill SJ, Ahrens S, Paulussen M, et al. Prognostic factors in Ewing's tumor of bone: analysis of 975 patients from the European Intergroup Cooperative Ewing's Sarcoma Study Group. J Clin Oncol 2000; 18:3108–14.
2. Atra A, Whelan JS, Calvagna V, et al. High-dose busulphan/melphalan with autologous stem cell rescue in Ewing's sarcoma. Bone Marrow Transplant 1997;20:843–6.
3. Diaz MA, Vicent MG, Madero L. High-dose busulfan/melphalan as conditioning for autologous PBPC transplantation in pediatric patients with solid tumors. Bone Marrow Transplant 1999;24:1157–9.
4. Bernstein ML, Devidas M, Lafreniere D, et al. Intensive therapy with growth factor support for patients with Ewing tumor metastatic at diagnosis: Pediatric Oncology Group/Children's Cancer Group Phase II Study 9457—a report from the Children's Oncology Group. J Clin Oncol 2006;24:152–9.
5. Engelhardt M, Zeiser R, Ihorst G, Finke J, Muller CI. High-dose chemotherapy and autologous peripheral

blood stem cell transplantation in adult patients with high-risk or advanced Ewing and soft tissue sarcoma. J Cancer Res Clin Oncol 2007;133:1–11.
6. McTiernan A, Driver D, Michelagnoli MP, Kilby AM, Whelan JS. High dose chemotherapy with bone marrow or peripheral stem cell rescue is an effective treatment option for patients with relapsed or progressive Ewing's sarcoma family of tumours. Ann Oncol 2006; 17:1301–5.
7. Grier HE, Krailo MD, Tarbell NJ, et al. Addition of ifosfamide and etoposide to standard chemotherapy for Ewing's sarcoma and primitive neuroectodermal tumor of bone. N Engl J Med 2003;348:694–701.
8. Kolb EA, Kushner BH, Gorlick R, et al. Long-term event-free survival after intensive chemotherapy for Ewing's family of tumors in children and young adults. J Clin Oncol 2003;21:3423–30.
9. Paulussen M, Ahrens S, Burdach S, et al. Primary metastatic (stage IV) Ewing tumor: survival analysis of 171 patients from the EICESS studies. European Intergroup Cooperative Ewing Sarcoma Studies. Ann Oncol 1998;9:275–81.
10. Bacci G, Ferrari S, Bertoni F, et al. Prognostic factors in nonmetastatic Ewing's sarcoma of bone treated with adjuvant chemotherapy: analysis of 359 patients at the Istituto Ortopedico Rizzoli. J Clin Oncol 2000; 18:4–11.
11. Rodriguez-Galindo C, Spunt SL, Pappo AS. Treatment of Ewing sarcoma family of tumors: current status and outlook for the future. Med Pediatr Oncol 2003;40:276–87.
12. Hayes FA, Thompson EI, Meyer WH, et al. Therapy for localized Ewing's sarcoma of bone. J Clin Oncol 1989;7:208–13.
13. Marina NM, Pappo AS, Parham DM, et al. Chemotherapy dose-intensification for pediatric patients with Ewing's family of tumors and desmoplastic small round-cell tumors: a feasibility study at St. Jude Children's Research Hospital. J Clin Oncol 1999;17:180–90.
14. Ohali A, Avigad S, Zaizov R, et al. Prediction of high risk Ewing's sarcoma by gene expression profiling. Oncogene 2004;23:8997–9006.
15. Cheung IY, Feng Y, Danis K, et al. Novel markers of subclinical disease for Ewing family tumors from gene expression profiling. Clin Cancer Res 2007;13: 6978–83.
16. Armengol G, Tarkkanen M, Virolainen M, et al. Recurrent gains of 1q, 8 and 12 in the Ewing family of tumours by comparative genomic hybridization. Br J Cancer 1997;75:1403–9.
17. Maurici D, Perez-Atayde A, Grier HE, Baldini N, Serra M, Fletcher JA. Frequency and implications of chromosome 8 and 12 gains in Ewing sarcoma. Cancer Genet Cytogenet 1998;100:106–10.
18. Hattinger CM, Potschger U, Tarkkanen M, et al. Prognostic impact of chromosomal aberrations in Ewing tumours. Br J Cancer 2002;86:1763–9.
19. Schaefer KL, Eisenacher M, Braun Y, et al. Microarray analysis of Ewing's sarcoma family of tumours reveals characteristic gene expression signatures associated with metastasis and resistance to chemotherapy. Eur J Cancer 2008;44:699–709.
20. Petricoin EF, Ardekani AM, Hitt BA, et al. Use of proteomic patterns in serum to identify ovarian cancer. Lancet 2002;359:572–7.
21. Suehara Y, Kondo T, Fujii K, et al. Proteomic signatures corresponding to histological classification and grading of soft-tissue sarcomas. Proteomics 2006;6: 4402–9.
22. Chen G, Gharib TG, Wang H, et al. Protein profiles associated with survival in lung adenocarcinoma. Proc Natl Acad Sci U S A 2003;100:13537–42.
23. Suehara Y, Kondo T, Seki K, et al. Pfetin as a prognostic biomarker of gastrointestinal stromal tumors revealed by proteomics. Clin Cancer Res 2008;14: 1707–17.
24. Okano T, Kondo T, Fujii K, et al. Proteomic signature corresponding to the response to gefitinib (Iressa, ZD1839), an epidermal growth factor receptor tyrosine kinase inhibitor in lung adenocarcinoma. Clin Cancer Res 2007;13:799–805.
25. Subong EN, Shue MJ, Epstein JI, Briggman JV, Chan PK, Partin AW. Monoclonal antibody to prostate cancer nuclear matrix protein (PRO:4-216) recognizes nucleophosmin/B23. Prostate 1999;39: 298–304.
26. Tanaka M, Sasaki H, Kino I, Sugimura T, Terada M. Genes preferentially expressed in embryo stomach are predominantly expressed in gastric cancer. Cancer Res 1992;52:3372–7.
27. Nozawa Y, Van Belzen N, Van der Made AC, Dinjens WN, Bosman FT. Expression of nucleophosmin/B23 in normal and neoplastic colorectal mucosa. J Pathol 1996;178:48–52.
28. Zhang Y. The ARF-B23 connection: implications for growth control and cancer treatment. Cell Cycle 2004;3:259–62.
29. Tsui KH, Cheng AJ, Chang PL, Pan TL, Yung BY. Association of nucleophosmin/B23 mRNA expression with clinical outcome in patients with bladder carcinoma. Urology 2004;64:839–44.
30. Wolf RE, Enneking WF. The staging and surgery of musculoskeletal neoplasms. Orthop Clin North Am 1996;27:473–81.
31. Shankar AG, Ashley S, Craft AW, Pinkerton CR. Outcome after relapse in an unselected cohort of children and adolescents with Ewing sarcoma. Med Pediatr Oncol 2003;40:141–7.
32. Urano F, Umezawa A, Yabe H, et al. Molecular analysis of Ewing's sarcoma: another fusion gene, EWS-E1AF, available for diagnosis. Cancer Sci 1998;89: 703–11.
33. Kondo T, Hirohashi S. Application of highly sensitive fluorescent dyes (CyDye DIGE Fluor saturation dyes) to laser microdissection and two-dimensional difference gel electrophoresis (2D-DIGE) for cancer proteomics. Nat Protoc 2006;1:2940–56.
34. Kaplan EL, Meier P. Nonparametric estimation from incomplete observations. J Am Stat Assoc 1958;53:1.
35. Cox DR. Regression models and life tables. J R Stat Soc 1972;34:187–220.
36. Obata H, Ueda T, Kawai A, et al. Clinical outcome of patients with Ewing sarcoma family of tumors of bone in Japan: the Japanese Musculoskeletal Oncology Group cooperative study. Cancer 2007;109: 767–75.
37. Yun JP, Miao J, Chen GG, et al. Increased expression of nucleophosmin/B23 in hepatocellular carcinoma and correlation with clinicopathological parameters. Br J Cancer 2007;96:477–84.
38. Bacci G, Ferrari S, Bertoni F, et al. Neoadjuvant chemotherapy for peripheral malignant neuroectodermal tumor of bone: recent experience at the Istituto Rizzoli. J Clin Oncol 2000;18:885–92.
39. Oberlin O, Deley MC, Bui BN, et al. Prognostic factors in localized Ewing's tumours and peripheral neuroectodermal tumours: the third study of the French Society of Paediatric Oncology (EW88 study). Br J Cancer 2001;85:1646–54.
40. Bailly RA, Bosselut R, Zucman J, et al. DNA-binding and transcriptional activation properties of the EWS-FLI-1 fusion protein resulting from the t(11;22) translocation in Ewing sarcoma. Mol Cell Biol 1994;14: 3230–41.
41. Sollazzo MR, Benassi MS, Magagnoli G, et al. Increased c-myc oncogene expression in Ewing's sarcoma: correlation with Ki67 proliferation index. Tumori 1999;85:167–73.
42. Javelaud D, Poupon MF, Wietzerbin J, Besancon F. Inhibition of constitutive NF-κB activity suppresses tumorigenicity of Ewing sarcoma EW7 cells. Int J Cancer 2002;98:193–8.
43. Fuchs B, Inwards CY, Janknecht R. Vascular endothelial growth factor expression is up-regulated by EWS-ETS oncoproteins and Sp1 and may represent an independent predictor of survival in Ewing's sarcoma. Clin Cancer Res 2004;10:1344–53.
44. Abudu A, Mangham DC, Reynolds GM, et al. Overexpression of p53 protein in primary Ewing's sarcoma of bone: relationship to tumour stage, response and prognosis. Br J Cancer 1999;79: 1185–9.
45. de Alava E, Antonescu CR, Panizo A, et al. Prognostic impact of P53 status in Ewing sarcoma. Cancer 2000;89:783–92.
46. Delattre O, Zucman J, Plougastel B, et al. Gene fusion with an ETS DNA-binding domain caused by chromosome translocation in human tumours. Nature 1992;359:162–5.
47. Ladanyi M. EWS-FLI1 and Ewing's sarcoma: recent molecular data and new insights. Cancer Biol Ther 2002;1:330–6.
48. Siligan C, Ban J, Bachmaier R, et al. EWS-FLI1 target genes recovered from Ewing's sarcoma chromatin. Oncogene 2005;24:2512–24.
49. Itahana K, Bhat KP, Jin A, et al. Tumor suppressor ARF degrades B23, a nucleolar protein involved in ribosome biogenesis and cell proliferation. Mol Cell 2003;12:1151–64.
50. Grisendi S, Mecucci C, Falini B, Pandolfi PP. Nucleophosmin and cancer. Nat Rev Cancer 2006; 6:493–505.

Int. J. Cancer: **124,** 2106–2115 (2009)

Transglutaminase 3 as a prognostic biomarker in esophageal cancer revealed by proteomics

Norihisa Uemura[1,2,3], Yukihiro Nakanishi[4], Hoichi Kato[2], Shigeru Saito[1,5], Masato Nagino[3], Setsuo Hirohashi[1] and Tadashi Kondo[1]*

[1]*Proteome Bioinformatics Project, National Cancer Center Research Institute, Tokyo, Japan*
[2]*Division of Esophageal Surgery, National Cancer Center Hospital, Tokyo, Japan*
[3]*Division of Surgical Oncology, Department of Surgery, Nagoya University Graduate School of Medicine, Nagoya, Japan*
[4]*Pathology Division, National Cancer Center Research Institute, Tokyo, Japan*
[5]*Chem and Bio Informatics Department, Infocom Corporation, Tokyo, Japan*

To develop a prognostic biomarker for esophageal squamous cell carcinoma (ESCC), we examined the proteomic profile of ESCC using two-dimensional difference gel electrophoresis (2D-DIGE), and identified proteins associated with prognosis by mass spectrometry. The prognostic performance of the identified proteins was examined by immunohistochemistry in additional cases. We identified 22 protein spots whose intensity was statistically different between ESCC cases with good ($N = 9$; survived more than 5 years without evidence of recurrence) and poor ($N = 24$; died within 2 years postsurgery) prognosis, within the patient group that had two or more lymph node metastases. Mass spectrometric protein identification resulted in 18 distinct gene products from the 22 protein spots. Transglutaminase 3 (TGM3) was inversely correlated with shorter patient survival. The prognostic performance of TGM3 was further examined by immunohistochemistry in 76 ESCC cases. The 5-year disease-specific survival rate was 64.5% and 32.1% for patients with TGM3-positive and TGM3-negative tumors, respectively ($p = 0.0033$). Univariate and multivariate analyses revealed that TGM3 expression was an independent prognostic factor among the clinicopathologic variables examined. It is noteworthy that the prognostic value of TGM3 was shown to be higher than those of the lymph node metastasis, intramural metastasis and vascular invasion status. These results establish TGM3 as a novel prognostic biomarker for ESCC for the first time. Examination of TGM3 expression may provide novel therapeutic strategies to prevent recurrence of ESCC.

Key words: esophageal cancer; prognosis; proteomics; TGM3 protein; two-dimensional difference gel electrophoresis

Esophageal cancer is the 8th most common cancer[1] and the 6th leading cause of cancer death worldwide.[2] Despite the use of modern surgical techniques in combination with radio- and chemotherapy, early recurrence is common and the overall 5-year survival rate remains below 40%.[3–5] Although the use of adjuvant and neoadjuvant chemotherapies has improved the survival times of esophageal cancer patients,[6] these treatment modalities cause serious side effects in a large number of patients and only benefit a limited number of patients in terms of overall survival times. On the other hand, 45–52% of patients with resectable esophageal cancer treated with surgery alone survive for more than 5 years.[7,8] The patients who can be completely cured by surgery alone receive unnecessary and harmful combination therapy. The response to treatment such as surgery or chemo-radiotherapy is variable, even when the patients are at the same clinical stage, and is not predicted by the existing diagnostic modalities. Accurate risk stratification is therefore of paramount importance to either avoid potential morbidity due to over-treatment or prevent further progression of disease.

Global mRNA expression studies have identified the gene clusters associated with the progression of esophageal cancer,[9–11] suggesting that multiple gene and protein alterations are implicated.[12] These alterations can be considered as potential biomarkers for detecting cancer, determining prognosis, and monitoring disease progression or therapeutic response. However, none of them has been proven to be clinically useful, and the response to treatment such as surgery or chemo-radiotherapy is not predicted by the existing diagnostic modalities. Practical biomarkers to predict response to treatment have long been desired to optimize therapeutic strategies and improve clinical outcomes.

The proteome is a functional translation of the genome. The genomic aberrations of cancer cells are transcribed to the transcriptome, translated to the proteome, then determining cancer phenotypes. In this sense, the proteome is a functional translation of the genome, directly regulating tumor behavior. It is obvious that proteomic features more directly reflect the tumor characters than genomic contents do. Proteomic studies can generate unique data about the final products of genome information. Many lines of evidence demonstrated discordance between mRNA and protein expression.[13–15] In addition, examining DNA sequences and measuring mRNA expression do not accurately predict the status of post-translational modifications such as phosphorylation and glycosylation, which play a key role in regulating the malignant behavior of cancer cells. Taken together, the proteome can be a rich source for biomarker identification.

In this study, we performed a proteomic study to identify biomarkers to predict the clinical outcome of esophageal squamous cell carcinoma (ESCC) patients. We used laser microdissection to recover tumor cells and neighboring normal epithelial cells from surgical specimens of esophageal cancer cases, and subjected the recovered cells to proteomic analysis using two-dimensional difference gel electrophoresis (2D-DIGE). We took particular note of postoperative prognosis in advanced esophageal cancer treated with surgery alone, and discovered prognostic biomarker candidates to optimize the existing surgical treatment strategy. As a result, transglutaminase 3 (TGM3) was identified as a prognostic biomarker candidate. The prognostic performance of TGM3 was successfully validated by immunohistochemistry in 76 additional ESCC cases. This is the first report concerning the prognostic value of TGM3 expression in ESCC. By measuring TGM3 expression in primary tumors, we will be able to refine the prognostic protocol and optimize current therapeutic strategies.

Material and methods

Patients and clinical information

We examined primary tumor tissues from 82 ESCC patients who underwent surgery at the National Cancer Center Hospital consecutively from 1998 to 2002. All patients underwent curative resection, and were not treated with chemo- or radiotherapy. The

Additional Supporting Information may be found in the online version of this article.

Grant sponsors: Ministry of Health, Labor and Welfare, National Cancer Institute of Biomedical Innovation of Japan (Promotion of Fundamental Studies), Foundation for Promotion of Cancer Research (Japan).

***Correspondence to:** Proteome Bioinformatics Project, National Cancer Center Research Institute, 5-1-1 Tsukiji, Chuo-ku, Tokyo 104-0045, Japan. Fax: +81-33-547-5298. E-mail: takondo@ncc.go.jp

Received 28 August 2008; Accepted after revision 15 October 2008
DOI 10.1002/ijc.24194
Published online 3 December 2008 in Wiley InterScience (www.interscience.wiley.com).

TABLE I – CLINICOPATHOLOGICAL DATA OF THE 58 ESOPHAGEAL CANCER CASES EXAMINED

	All cases	Good prognosis group	Poor prognosis group	*p*
Number of cases	58	34	24	
Age (mean ± SD) (yr)	62.3 ± 8.4	59.9 ± 9.5	63.0 ± 6.3	0.447
Gender				0.015[1]
Male	50	26	24	
Female	8	8	0	
Histologic differentiation				0.416
Well differentiated	21	15	6	
Moderately differentiated	25	14	11	
Poorly differentiated	12	5	7	
Tumor location				0.316
Upper	5	2	4	
Middle	25	13	12	
Lower	28	20	8	
Macroscopic classification				0.974
1	1	1	0	
2	34	20	14	
3	23	13	10	
Tumor size (mean ± SD) (cm)	6.2 ± 2.2	6.0 ± 1.9	6.4 ± 2.4	0.673
Number of LN metastases				<0.001[1]
0	13	13	0	
1	12	12	0	
2	5	1	4	
3	7	2	5	
≥4	21	6	15	
SCC (mean ± SD) (ng/ml)	1.5 ± 1.5	1.3 ± 1.2	1.7 ± 1.7	0.303
CEA (mean ± SD) (ng/ml)	3.0 ± 1.4	2.8 ± 1.1	3.3 ± 1.8	0.200
Lymphatic invasion				0.025[1]
Negative	22	16	6	
Positive	36	18	18	
Vascular invasion				0.024[1]
Negative	20	16	4	
Positive	38	18	20	
Intramural metastasis				0.007[1]
Absent	50	33	17	
Present	8	1	7	
Prognosis				
Good prognosis group[2]	34			
Poor prognosis group[3]	24			

[1]Considered to be significant ($p < 0.05$).–[2]Survived more than 5 years without evidence of recurrence.–[3]Died within 2 years postsurgery.

patients were newly diagnosed with thoracic ESCC and were followed up for at least 5 years after surgery. The overall clinicopathological data of the cases are summarized in Table I, while information on the individual cases is available in Supplemental Table S1. Two or three tissue fragments, less than 10 mm^3 in volume, were grossly obtained from primary tumors. Matched normal mucosal tissues located at least 5 cm away from the tumor margins were also included in this study. The resected tissues were snap-frozen in liquid nitrogen and stored at −80°C until use. The recovered specimens were histologically examined and the clinicopathological stage was determined according to the International Union against Cancer tumor-node-metastasis (TNM) classification.[16] All cases were classified as T3N0-1M0. This study was approved by the ethics committee of the National Cancer Center and written informed consent was obtained from the patients.

The patients that survived more than 5 years without evidence of recurrence were categorized in the good prognosis group (N = 39) while the patients that died within 2 years post surgery were categorized in the poor prognosis group (N = 28). The proteomic profiles of these two sample groups were compared.

We performed immunohistochemistry on 76 cases, which included 14 cases that were not categorized in either group. The clinicopathological data of the 76 esophageal cancer cases are demonstrated in Table II.

Laser microdissection

Specific cell populations were recovered by laser microdissection according to our previous reports[17,18] (Fig. 1*a*). A 1 mm^2 of microdissected area, recorded during microdissection, was recovered from hematoxylin-stained tissues for each 2D-DIGE gel. As tumor tissues could not be recovered in 9 cases (Supplemental Table S1) because of poor preservation, we finally examined 58 tumor tissues and 53 normal epithelium tissues.

2D-DIGE and image analysis

2D-DIGE was performed as previously described.[17,18] In brief, a common internal control sample was created by mixing a small portion of all protein samples used in this study, which was labeled with Cy3 fluorescent dye (CyDye DIGE Fluor saturation dye, GE Healthcare Biosciences, Uppsala, Sweden). Individual samples were labeled with Cy5 fluorescent dye (CyDye DIGE Fluor saturation dye, GE Healthcare Biosciences). These differently labeled protein samples were mixed together and separated by two-dimensional gel electrophoresis (2D-PAGE) according to their isoelectric point and molecular weight. The first dimension separation was achieved using a 24 cm-length immobiline gel (IPG, pI 4–7, GE Healthcare Biosciences) and Multiphor II (GE Healthcare Biosciences), while the second dimension separation using a home-made gradient gel with GiantGelRunner (Biocraft, Tokyo, Japan), with a separation distance of 36 cm. The gels were scanned using a laser scanner (Typhoon Trio, GE Healthcare Biosciences) at the appropriate wavelength for Cy3 or Cy5. For all protein spots, the Cy5 intensity was normalized with the Cy3 intensity in the same gel using the Progenesis SameSpots software version 3 (Nonlinear Dynamics, Newcastle, UK), so that gel-to-gel variations were canceled out (Fig. 1*b*). We monitored the system reproducibility by running the same sample twice (case 15; Supplemental Table S1). The scatter plot showed that the intensity

TABLE II – UNIVARIATE AND MULTIVARIATE ANALYSIS OF PROGNOSTIC FACTORS AND RELATIONSHIP BETWEEN CLINICOPATHOLOGIC VARIABLES AND TGM3 EXPRESSION

Variable	Number of cases	Disease-specific survival		Multivariate analysis of tumor-specific survival by Cox regression			TGM3 positive (no. cases)	TGM3 negative (no. cases)	Correlation with TGM3 expression p value[2]
		5 yr (%)	Log-rank (P)	p	Relative risk	95% CI			
All cases	76	52.6					48	28	
Age (yr)			0.4599						0.345
<65	42	57.1					29	13	
≥65	34	47.1					19	15	
Gender			0.0597						0.548
Male	64	48.4					9	3	
Female	12	75.0					39	25	
Histologic differentiation			0.1551						0.884
Well	25	64.0					15	10	
Nonwell	51	47.0					33	18	
Tumor location			0.5276						0.198
Upper	5	40.0					5	0	
Middle, lower	71	53.5					43	28	
Macroscopic classification			0.5805						0.079
1, 2	43	55.8					23	20	
3	33	48.3					25	8	
Tumor size (cm)			0.5669						0.311
<6.0	37	56.6					26	11	
≥6.0	39	48.7					22	17	
Pathologic N status			0.0013[1]	0.025[1]	4.101	1.197–14.044			0.527
pN0	18	88.9					13	5	
pN1	58	41.3					35	23	
SCC (ng/ml)			0.3090						0.987
≤1.5	61	55.7					38	23	
>1.5	15	40.0					10	5	
CEA (ng/ml)			0.1402						0.548
≤5	67	55.2					41	26	
>5	9	29.6					7	1	
Lymphatic invasion			0.0084[1]	0.351	1.472	0.654–3.313			0.450
Negative	30	70.0					21	9	
Positive	46	41.2					27	19	
Vascular invasion			0.0082[1]	0.228	1.608	0.743–3.478			0.158
Negative	31	74.2					23	8	
Positive	45	37.8					25	20	
Intramural metastasis			0.0072[1]	0.778	1.142	0.452–2.884			0.229
Absent	68	57.3					45	23	
Present	8	12.5					3	5	
TGM3			0.0033[1]	0.015[1]	0.430	0.218–0.848			
Negative	28	32.1							
Positive	48	64.5							

Abbreviation: 95% CI, 95% confidence interval.
[1]Considered to be significant ($p < 0.05$).–[2]Fisher's exact test for categorical variables and Mann-Whitney U test for continuous variables.

value of 95% of protein spots was scattered within a 2-fold value difference, and that the correlation coefficient was 0.8352, demonstrating the high reproducibility of our profiling method (Fig. 1*c*). The spot intensity data were exported from the Progenesis SameSpots software as Excel files, amenable to data analysis.

Data analysis

As a preprocess of data analysis, raw intensity data for each experiment were log2 transformed and then Z score transformation was applied to standardize the distribution of the intensity data.[19] Hierarchical clustering was performed with the Euclidean distance and unweighted pair group methods, using the arithmetic average (UPGMA) method on the standardized data to reveal the global features of the proteomic profiles acquired. To identify the spots that had different intensity between the 2 groups, the z-test was used for each spot. As the obtained p-value list possibly included false positive results due to multiple tests, we estimated the false discovery rate (FDR) following the Benjamini-Hochberg procedure according to the previous report.[20] We subsequently selected the spots so that the FDR is less than 0.05. For the comparison of normal tissues with tumors, we chose the spots the intensity ratio of group means was at least 4 times above the aforementioned FDR criteria.

Mass spectrometric protein identification

The proteins corresponding to the protein spots detected were identified by mass spectrometry according to our previous report.[21] Cy5-labeled proteins separated by 2D-PAGE were recovered in gel plugs and digested with modified trypsin (Promega, Madison, WI). The trypsin digests were subjected to liquid chromatography coupled with tandem mass spectrometry, a Finnigan LTQ linear ion trap mass spectrometer (Thermo Electron, San Jose, CA) equipped with a nano-electrospray ion source (AMR, Tokyo, Japan). The Mascot software (version 2.1, Matrix science, London, UK) was used to search for the mass of the peptide ion peaks against the SWISS-PROT database (*Homo sapiens*, 16,529 sequence in Sprot_52.5 fasta file). Proteins with a Mascot score of 34 or more were subjected to protein identification. When multiple proteins were identified in a single spot, the proteins with the highest number of peptides were considered as those corresponding to the spot.

Pathway analysis of expression data

Pathway analysis of the protein expression pattern was performed using the MetaCore software (GeneGo, St. Joseph, MI). MetaCore identifies networks based on a manually curated

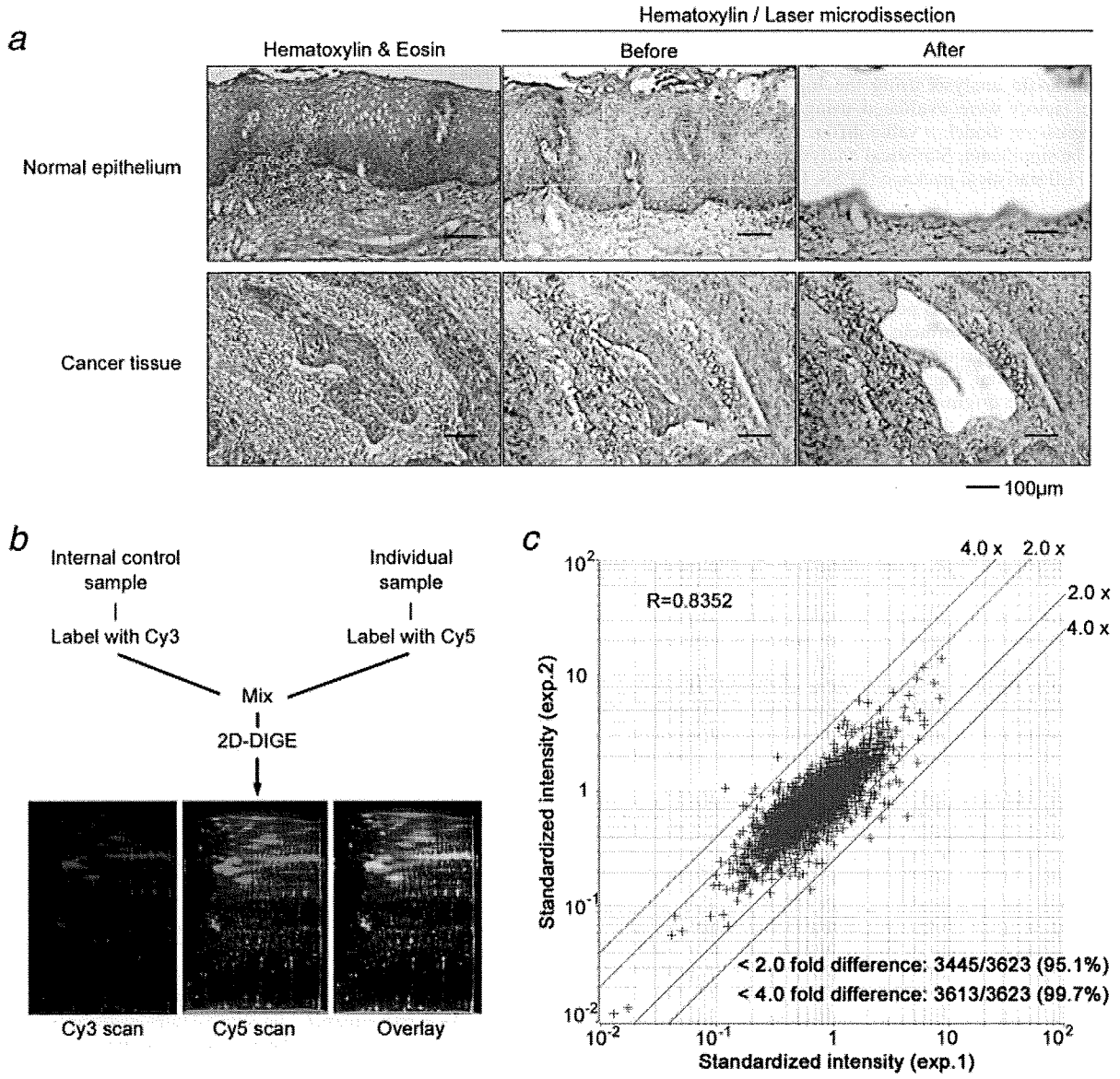

FIGURE 1 – (*a*) Laser microdissection of ESCC. Tissue sections were stained with hematoxylin and eosin for histological observation, while neighboring serial sections were stained with hematoxylin alone for the proteomic study. (*b*) The extracted proteins were labeled with fluorescent dyes and separated by 2D-DIGE. (*c*) Scattergram of 2 independent experiments demonstrating the high reproducibility of 2D-DIGE.

database containing known molecular interactions, functions, and disease interrelationships using proteome data sets. The pathways are identified by the probability that a random set of proteins the same size as the input list would give rise to a particular mapping by chance.

Immunohistochemistry and tissue microarray

Immunohistochemical staining for TGM3 was performed on methanol-fixed, paraffin-embedded tissue sections from 76 cases (Supplemental Table S1) using the Dako REAL EnVision Detection System (DAKO, Glostrup, Denmark) following the manufacturer's instructions. The sections were deparaffinized, dehydrated and blocked by 3 mL/L H_2O_2 in methanol for 30 min to remove endogenous peroxidase activity. The sections were autoclaved in 10 mM citrate buffer (pH 6.0) at 121°C for 10 min. The primary antibody used was a rabbit polyclonal, mono-specific antibody against TGM3 (HPA004728; Atlas antibodies, Stockholm, Sweden) at a dilution of 1:100. One pathologist (Y. N.) and one medical doctor (N. U.) reviewed the sections stained with anti-TGM3 antibody in a blinded fashion regarding clinical data. The normal esophageal epithelium served as an internal positive control. Cases in which more than 10% tumor cells were positively stained with anti-TGM3 antibody were considered as TGM3 positive, while cases with less than 10% TGM3 positive tumor cells were considered as a TGM3 negative. Staining was evaluated at the dominant differentiation area of the tumor if considerable tumor heterogeneity was present.

We examined TGM3 expression using our home-made tissue microarray containing 59 normal tissues and 323 tumor tissues (Supplemental Table S2).

Statistical analysis

The correlation between TGM3 expression and clinicopathological features was evaluated using the Fisher's exact test for categorical variables and the Mann-Whitney *U* test for continuous variables. The disease-specific survival time was calculated from the

first resection of the primary tumor to death of disease-specific causes. All time-to-event end points were computed by the Kaplan-Meier method.[22] Potential prognostic factors were identified by univariate analysis using the log-rank test. Independent prognostic factors were evaluated using the Cox's proportional hazards regression model. p value differences of <0.05 were considered to be significant. Statistical analyses were performed using the SPSS 11.0 statistical package (SPSS, Chicago, IL).

Results

2D-DIGE generated quantitative expression profiles that included 3,623 protein spots per sample. Based on the overall similarity of the acquired protein expression profiles, the samples were divided into 2 groups: tumor tissues and normal epithelial tissues (Supplemental Fig. S1); that is, the proteomic profiles reflected the tissue origin of the sample. Considerable differences were observed between the proteomic profile of tumors and normal tissues; we found 200 protein spots that matched the criteria of an FDR < 0.001 and a fold difference >4 between the tissue groups. The intensity of 33 of these spots indicated increased protein expression levels while the remaining 167 spots indicated decreased expression in tumor tissues. All proteins corresponding to these 200 protein spots were identified (Supplemental Table S3).

The samples were not grouped according to the prognosis group to which they belonged based on their overall protein expression features. Similarly, no protein spots with significantly different intensity between these two groups were observed. However, the gender, the number of lymph node metastases, the lymphatic and vascular invasion status, and the intramural metastasis status were significantly different between the patients groups with different prognosis (Table I).

The number of lymph node metastases is one of the major prognostic factors in esophageal cancer.[23] We classified the patients based on their lymph node metastasis status into the good and bad prognosis group, and found 22 protein spots with significantly different intensity between the two groups (FDR < 0.05). The localization of the 22 spots on the two-dimensional image is shown in Figure 2*a* (enlarged image in Supplemental Fig. S2). Mass spectrometric protein identification revealed that the 22 protein spots corresponded to 18 distinct gene products (Table III, Fig. 2*b* and Supplemental Table S4). Pathway analysis using a MetaCore software analysis tool showed that 17 of the 18 identified proteins were part of a network (Fig. 2*c*) in which STAT1, p53 and HNF4 seemed to be key proteins. TGM3 was connected to STAT1 through Sp1, which directly regulates TGM3 expression[24] and is an intermediary of p53, which is known to be a prognostic factor of several malignancies including esophageal cancer.[25] TGM3 spots seemed 3 times in the list of the 22 protein spots with consistently lower intensity in the poor prognosis group.

To further validate the prognostic value of TGM3 expression in ESCC, we examined the expression of TGM3 in 76 ESCC cases using immunohistochemistry. Both cytoplasmic and nuclear TGM3 staining were observed, depending on the case (Fig. 3*a*, enlarged image in Supplemental Fig. S3), although only the former has been reported previously[26,27] and was considered as indicating positive staining in this study.

The 5-year disease-specific survival rate was significantly higher in the 48 TGM3-positive compared with the 28 TGM3-negative cases (64.5 *versus* 32.1%; $p = 0.0033$; Fig. 3*b*, Table II). Multivariate analysis revealed that TGM3 expression was an independent predictor of disease-specific survival (Table II). The immunohistochemical expression of TGM3 did not correlate with any other clinicopathological variables (Table II).

In tissue microarray analysis, TGM3 was shown to be expressed in all normal squamous epithelia and squamous cell carcinomas examined, including those arising in the skin, lung, oral cavity and uterus. In addition, TGM3 was expressed in a few cases of nonsquamous epithelia and nonsquamous cell carcinomas, including those arising in the breast, prostate and thyroid gland (Fig. 3*c*).

Discussion

A variety of treatments is currently available for esophageal cancer.[6] The choice of treatment is crucial, as the response is diverse between the patients, even when they are diagnosed at the same clinical stage.[6] Treatment-related complications may easily lead to serious and occasionally fatal adverse reactions, such as myocardial infarction, heart failure, and pneumonia.[28,29] Therefore, by predicting response to treatment and optimizing individualized therapy, we will be able to improve the clinical outcome of esophageal cancer patients.

Novel prognostic modalities have long been desired to improve the management of ESCC. Global genomic and transcriptomic expression studies have been conducted to detect prognostic molecular biomarkers for ESCC.[30,31] However, these studies did not result in the identification of novel practical biomarkers, because they used too many molecules to predict clinical outcome, and did not perform sufficient verification experiments in clinical-scale sample sets using practical methods such as immunohistochemistry. Although proteomics has much potential to reveal the molecular background of esophageal cancer, this is the first report to employ proteomics to identify prognostic biomarkers in esophageal cancer, and to successfully establish TGM3 as a single prognostic biomarker.

The prognosis of esophageal cancer patients may be affected by various factors, including those used in TNM classification and the presence of intramural metastasis and vascular invasion.[29] Therefore, the molecular background of tumors from patients with similar prognosis could vary even when they have the same T and M stage, as in this study. Indeed, we did not identify any protein spots with different intensity between the good and poor prognosis groups. We assumed that this was probably due to the high heterogeneity of the molecular background of the tumors. With this notion, we subsequently focused our analysis on comparing the proteomic profiles of patients with different survival periods within the patient group that had two or more lymph node metastases at the time of pathological diagnosis. This analysis is clinically significant because this patient group generally has poor prognosis and is in more need of the development of suitable prognostic biomarkers. As a consequence, we successfully identified 22 protein spots that had different intensity between the aforementioned patient subgroups. These observations suggest that following a strategy that is based on the use of such clinically relevant parameters is an effective way to identify the proteins that correlate with the malignant potential of tumors.

We identified 18 proteins of prognostic value in the primary tumors. Network analysis revealed that 17 of them were linked through the STAT1, p53 and HNF4 transcription factors, all of which are aberrantly regulated in esophageal cancer. Suppression of the EGF-STAT1 pathway leads to progression of esophageal cancer.[32] p53 immunoreactivity has been detected in 34–67% of ESCC cases,[33–36] and is significantly correlated with cancer-specific death.[25] HNF4alpha expression significantly correlates with MUC4 expression,[37] which is a mediator of tumor growth and metastasis by acting as a ligand for the ErbB2 tyrosine kinase receptor.[38–40] These observations suggest that a limited number of transcription factors may affect a large number of genes, resulting in poor prognosis for esophageal cancer.

We considered that TGM3 was a strong prognostic biomarker candidate, because its immunohistochemical expression clearly correlated with clinical outcome in our study and it has also been shown to be potentially relevant to ESCC.[27] TGM3 expression has been previously correlated with certain malignant phenotypes in ESCC. Liu *et al.* reported TGM3 expression and histological grade are inversely correlated in ESCC,[27] while it should be noted that Mendez *et al.* reported that TGM3 expression is inversely

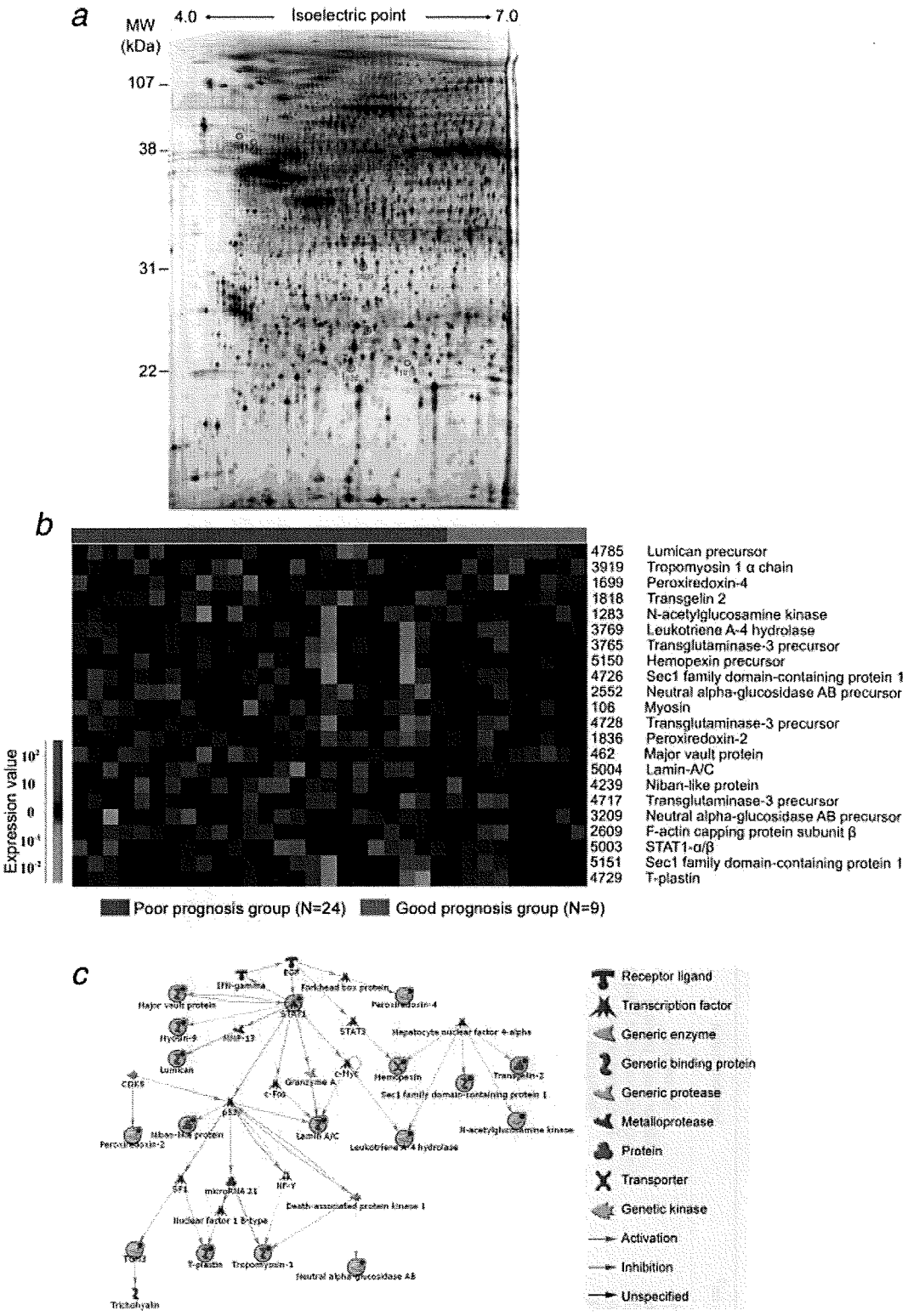

FIGURE 2 – Identification of proteins differentially expressed in ESCC. (*a*) A representative two-dimensional gel image showing the localization of proteins of ESCC tissues. The 22 spots identified in this study are circled and numbered. The spot numbers correspond to those in Figure 2*b*, Table III, and Supplemental Table S2. The image is shown enlarged in Supplemental Figure S2. (*b*) Hierarchical clustering of the 33 ESCC cases based on the intensity of the 22 protein spots. Purple, poor prognosis group; brown, good prognosis group. Right, spot numbers and protein names. (*c*) Pathway analysis of the identified proteins. Seventeen of eighteen of the identified proteins were shown to be part of a network by pathway analysis using the MetaCore software analysis tool.

TABLE III – LIST OF THE IDENTIFIED PROTEINS

Spot no.[1]	Accession no.[2]	Identified protein	z-value	*p*-value	FDR	Overall rank	pI (cal)[3]	MW (cal; kD)[3]	Protein score[4]	Peptide matches	Sequence coverage (%)
106	P35579	Myosin-9	−3.99	6.70E-05	2.85E-02	8	5.5	227.6	420	8	3.8
462	Q14764	Major vault protein	−3.85	1.18E-04	3.33E-02	12	5.34	99.6	88	2	4.8
1283	Q9UJ70	*N*-acetylglucosamine kinase	−4.94	7.85E-07	1.42E-03	2	5.81	37.7	97	2	6.1
1699	Q13162	Peroxiredoxin-4	3.69	2.21E-04	3.80E-02	21	5.86	30.7	186	4	13.7
1818	P37802	Transgelin-2	−6.51	7.47E-11	2.71E-07	1	8.41	22.5	228	3	18.6
1836	P32119	Peroxiredoxin-2	−3.95	7.86E-05	2.85E-02	10	5.66	22	211	4	24.2
2552	Q14697	Neutral alpha-glucosidase AB precursor	−4.03	5.51E-05	2.85E-02	7	5.74	107.3	137	2	3.4
2609	P47756	F-actin capping protein subunit beta	−3.73	1.89E-04	3.80E-02	17	5.36	31.6	224	3	13.4
3209	Q14697	Neutral alpha-glucosidase AB precursor	−3.75	1.74E-04	3.80E-02	16	5.74	107.3	419	9	12.1
3765	Q08188	Transglutaminase-3	−4.36	1.29E-05	1.17E-02	4	5.62	76.9	888	16	24
3769	P09960	Leukotriene A-4 hydrolase	−4.64	3.52E-06	4.26E-03	3	5.8	69.9	702	12	20.5
3919	P09493	Tropomyosin-1 alpha chain	3.73	1.90E-04	3.80E-02	18	4.69	32.7	104	2	6.7
4239	P02545	Lamin-A/C	−3.83	1.31E-04	3.38E-02	14	6.57	74.4	282	4	7.7
4717	Q08188	Transglutaminase-3	−3.76	1.67E-04	3.80E-02	15	5.62	76.9	133	2	2.7
4726	P02790	Hemopexin precursor	−4.09	4.39E-05	2.65E-02	6	6.55	52.4	159	4	6.7
4728	Q08188	Transglutaminase-3	−3.95	7.77E-05	2.85E-02	9	5.62	76.9	535	10	14.6
4729	P13797	T-plastin	−3.61	3.02E-04	4.98E-02	22	5.52	70.9	122	3	5.3
4785	P51884	Lumican precursor	3.89	9.91E-05	3.27E-02	11	6.16	38.7	159	3	8.6
5003	P42224	Signal transducer and activator of transcription 1-alpha/beta	−3.71	2.07E-04	3.80E-02	19	5.74	87.9	114	3	4.3
5004	Q96TA1	Niban-like protein 1	−3.85	1.20E-04	3.33E-02	13	5.81	83.1	292	5	10.8
5150	Q8WVM8	Sec1 family domain-containing protein 1	−4.10	4.10E-05	2.65E-02	5	5.89	72.7	115	2	3.7
5151	Q8WVM8	Sec1 family domain-containing protein 1	−3.70	2.15E-04	3.80E-02	20	5.89	72.7	94	3	8.7

[1]Spot numbers refer to those in Figure 1A and Supplemental Figure 1.–[2]Accession numbers of proteins were derived from Swiss-Prot and NCBI nonredundant databases.–[3]Theoretical isoelectric point and molecular weight obtained from Swiss-Prot and the ExPASy database. (http://au.expasy.org).–[4]Mascot score for the identified proteins based on the peptide ions score ($p < 0.05$) (http://www.matrixscience.com).

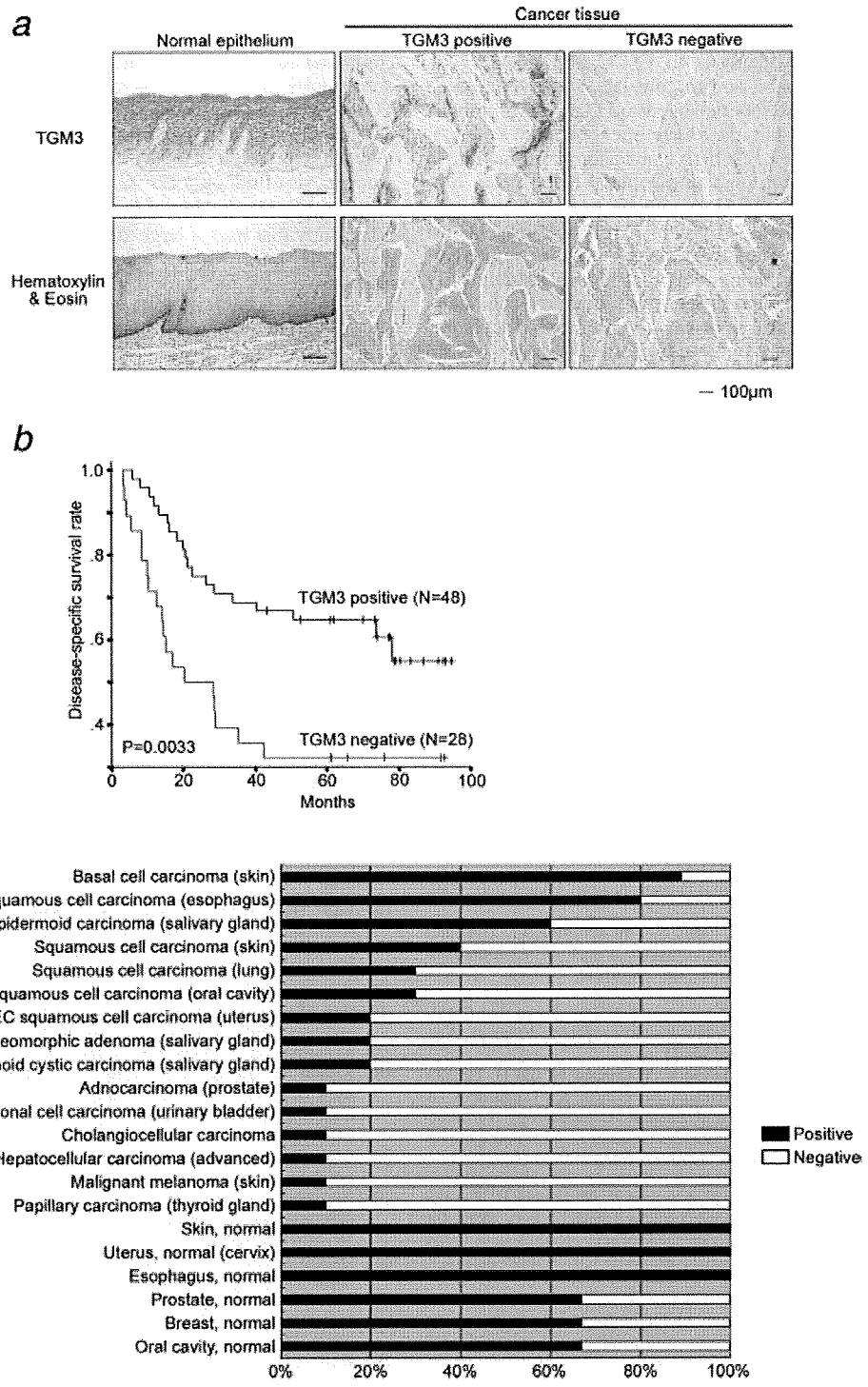

FIGURE 3 – Validation of the differential expression of TGM3 in relation to prognosis. (*a*) Immunohistochemistry; TGM3 was expressed in all normal esophageal epithelia and 63% cancer tissues. The image is shown enlarged in Supplemental Figure S3. (*b*) Kaplan-Meier survival curves for ESCC patients in relation to TGM3 expression. Patients with positive TGM3 expression had significantly better ($p = 0.0033$) prognosis than patients with negative TGM3 expression. (*c*) Tissue microarray data. TGM3 was expressed in normal squamous epithelia and squamous cell carcinomas arising in a range of tissues (a detailed list is shown in Supplemental Table 2), and some adenocarcinomas and their normal counterparts.

correlated with lymph node metastasis of oral squamous cell carcinoma.[41] Although Liu *et al.* reported that TGM3 expression correlated with histological grade in ESCC,[27] we did not observe any correlation between TGM3 expression and the clinico-pathological parameters examined, including the tumor stage. This discordance is probably due to the different antibody used, the different surgical procedure followed,[42] and the different clinical background of the patients included in the studies. A multi-institutional

validation study that will take into account such differences will be required to firmly establish TGM3 as a practical prognostic biomarker. In oligomicroarray analysis in ESCC, the TGM3 gene was reported to be suppressed and to correlate with lymph node metastasis.[31] Although these reports suggested that TGM3 may be involved in cancer progression, they have not shown the prognostic or other practical value of TGM3 expression examination in ESCC. Genome and transcriptome studies have listed many biomarker candidates included TGM3,[31] without, however, detecting or proposing single biomarkers of potential practical use. In this study, we detected the proteins associated with the survival of ESCC patients using a proteomic approach, and subsequently selected TGM3 as an individual prognostic biomarker candidate. We then showed that the positive or negative immunohistochemical expression of TGM3 in our study corresponds to TGM3 expression as assessed by the proteomics tools we employed, and thus can be used to assess the expression level of TGM3 (Fig. 3*a*) in practice.

TGM3 plays a key role in epidermal terminal differentiation through cross-linking structural proteins such as involucrin, loricrin and small proline-rich proteins.[43] Although the role of TGM3 has been well established in the differentiation of skin keratinocytes,[44] little information is available concerning its involvement in esophageal epithelium. TGM3 stabilizes the cornified envelope of cells, a process that precedes the transition of keratinocytes to corneocytes by apoptosis. Therefore, down-regulation of TGM3 in ESCC may interrupt the potentially critical initiation of apoptosis, thereby favoring tumor cell survival.

TGM3 expression was decreased in ESCC tissues compared with normal tissues; all normal tissues strongly expressed TGM3 compared to only 63% of the ESCC tissues. This observation is consistent with previous microarray studies[45,46] that indicated that TGM3 is down-regulated in many types of malignancies compared with the corresponding normal tissues, suggesting that the reduced expression of TGM3 may play a common role in the carcinogenesis of not only ESCC but also other carcinomas.

In conclusion, we performed the first esophageal cancer proteomics study that uses a large-scale clinical sample set that includes prognostic information, and identified TGM3 expression as a novel prognostic indicator in ESCC. The use of a common internal control sample in 2D-DIGE, and the use of laser microdissection contributed to accurate protein expression profiling. The immunohistochemical examination of TGM3 expression may help identify patients with high risk for recurrence, and may improve the clinical outcome of these patients through closer postoperative follow-up and additional treatment. Our results therefore provide the possibility for the development of novel strategies for ESCC management.

Acknowledgements

The excellent technical support of Ms. Yukiko Kobori and Ms. Mina Fujishiro in electrophoresis and Ms. Satoko Kouda in the immunohistochemical study are greatly appreciated. Norihisa Uemura is a recipient of a Research Resident Fellowship from the Foundation for Promotion of Cancer Research (Japan) within the framework of the 3rd Term Comprehensive 10-Year Strategy for Cancer Control.

References

1. Parkin DM, Pisani P, Ferlay J. Estimates of the worldwide incidence of 25 major cancers in 1990. Int J Cancer 1999;80:827–41.
2. Pisani P, Parkin DM, Bray F, Ferlay J. Estimates of the worldwide mortality from 25 cancers in 1990. Int J Cancer 1999;83:18–29.
3. Ilson DH. Oesophageal cancer: new developments in systemic therapy. Cancer Treat Rev 2003;29:525–32.
4. Enzinger PC, Mayer RJ. Esophageal cancer. N Engl J Med 2003;349: 2241–52.
5. Mariette C, Balon JM, Piessen G, Fabre S, Van Seuningen I, Triboulet JP. Pattern of recurrence following complete resection of esophageal carcinoma and factors predictive of recurrent disease. Cancer 2003;97:1616–23.
6. Shinoda M, Hatooka S, Mori S, Mitsudomi T. Clinical aspects of multimodality therapy for resectable locoregional esophageal cancer. Ann Thorac Cardiovasc Surg 2006;12:234–41.
7. Ando N, Iizuka T, Kakegawa T, Isono K, Watanabe H, Ide H, Tanaka O, Shinoda M, Takiyama W, Arimori M, Ishida K, Tsugane S. A randomized trial of surgery with and without chemotherapy for localized squamous carcinoma of the thoracic esophagus: the Japan Clinical Oncology Group Study. J Thorac Cardiovasc Surg 1997;114:205–9.
8. Ando N, Iizuka T, Ide H, Ishida K, Shinoda M, Nishimaki T, Takiyama W, Watanabe H, Isono K, Aoyama N, Makuuchi H, Tanaka O, et al. Surgery plus chemotherapy compared with surgery alone for localized squamous cell carcinoma of the thoracic esophagus: a Japan Clinical Oncology Group Study–JCOG9204. J Clin Oncol 2003;21: 4592–6.
9. Tamoto E, Tada M, Murakawa K, Takada M, Shindo G, Teramoto K, Matsunaga A, Komuro K, Kanai M, Kawakami A, Fujiwara Y, Kobayashi N, et al. Gene-expression profile changes correlated with tumor progression and lymph node metastasis in esophageal cancer. Clin Cancer Res 2004;10:3629–38.
10. Kan T, Shimada Y, Sato F, Ito T, Kondo K, Watanabe G, Maeda M, Yamasaki S, Meltzer SJ, Imamura M. Prediction of lymph node metastasis with use of artificial neural networks based on gene expression profiles in esophageal squamous cell carcinoma. Ann Surg Oncol 2004;11:1070–8.
11. Gomes LI, Esteves GH, Carvalho AF, Cristo EB, Hirata R, Jr, Martins WK, Marques SM, Camargo LP, Brentani H, Pelosof A, Zitron C, Sallum RA, et al. Expression profile of malignant and nonmalignant lesions of esophagus and stomach: differential activity of functional modules related to inflammation and lipid metabolism. Cancer Res 2005;65:7127–36.
12. Vallbohmer D, Lenz HJ. Predictive and prognostic molecular markers in outcome of esophageal cancer. Dis Esophagus 2006;19:425–32.
13. Chen G, Gharib TG, Huang CC, Taylor JM, Misek DE, Kardia SL, Giordano TJ, Iannettoni MD, Orringer MB, Hanash SM, Beer DG. Discordant protein and mRNA expression in lung adenocarcinomas. Mol Cell Proteomics 2002;1:304–13.
14. Varambally S, Yu J, Laxman B, Rhodes DR, Mehra R, Tomlins SA, Shah RB, Chandran U, Monzon FA, Becich MJ, Wei JT, Pienta KJ, et al. Integrative genomic and proteomic analysis of prostate cancer reveals signatures of metastatic progression. Cancer Cell 2005;8:393–406.
15. Gygi SP, Rochon Y, Franza BR, Aebersold R. Correlation between protein and mRNA abundance in yeast. Mol Cell Biol 1999;19:1720–30.
16. Sobin L, Wittekind C. UICC TNM Classification of malignant tumors, 6th edn. New York: Wiley-Liss, 2002.
17. Kondo T, Seike M, Mori Y, Fujii K, Yamada T, Hirohashi S. Application of sensitive fluorescent dyes in linkage of laser microdissection and two-dimensional gel electrophoresis as a cancer proteomic study tool. Proteomics 2003;3:1758–66.
18. Kondo T, Hirohashi S. Application of highly sensitive fluorescent dyes (CyDye DIGE Fluor saturation dyes) to laser microdissection and two-dimensional difference gel electrophoresis (2D-DIGE) for cancer proteomics. Nat Protoc 2006;1:2940–56.
19. Cheadle C, Vawter MP, Freed WJ, Becker KG. Analysis of microarray data using Z score transformation. J Mol Diagn 2003;5:73–81.
20. Benjamini Y, Hochberg Y. Controlling the false discovery rate: a practical and powerful approach to multiple testing. J R Stat Soc B 1995;57:289–300.
21. Okano T, Kondo T, Kakisaka T, Fujii K, Yamada M, Kato H, Nishimura T, Gemma A, Kudoh S, Hirohashi S. Plasma proteomics of lung cancer by a linkage of multi-dimensional liquid chromatography and two-dimensional difference gel electrophoresis. Proteomics 2006;6: 3938–48.
22. Kaplan E, Meier P. Nonparametric estimation from incomplete observations. J Am Stat Assoc 1958;53:457–81.
23. Tachibana M, Kinugasa S, Yoshimura H, Shibakita M, Tonomoto Y, Dhar DK, Nagasue N. Clinical outcomes of extended esophagectomy with three-field lymph node dissection for esophageal squamous cell carcinoma. Am J Surg 2005;189:98–109.
24. Lee JH, Jang SI, Yang JM, Markova NG, Steinert PM. The proximal promoter of the human transglutaminase 3 gene. Stratified squamous epithelial-specific expression in cultured cells is mediated by binding of. Sp1 and ets transcription factors to a proximal promoter element. J Biol Chem 1996;271:4561–8.
25. Aloia TA, Harpole DH, Jr, Reed CE, Allegra C, Moore MB, Herndon JE, II, D'Amico TA. Tumor marker expression is predictive of survival in patients with esophageal cancer. Ann Thorac Surg 2001;72: 859–66.
26. Hitomi K, Presland RB, Nakayama T, Fleckman P, Dale BA, Maki M. Analysis of epidermal-type transglutaminase (transglutaminase 3)

in human stratified epithelia and cultured keratinocytes using monoclonal antibodies. J Dermatol Sci 2003;32:95–103.
27. Liu W, Yu ZC, Cao WF, Ding F, Liu ZH. Functional studies of a novel oncogene TGM3 in human esophageal squamous cell carcinoma. World J Gastroenterol 2006;12:3929–32.
28. Ishikura S, Nihei K, Ohtsu A, Boku N, Hironaka S, Mera K, Muto M, Ogino T, Yoshida S. Long-term toxicity after definitive chemoradiotherapy for squamous cell carcinoma of the thoracic esophagus. J Clin Oncol 2003;21:2697–702.
29. Igaki H, Kato H, Tachimori Y, Sato H, Daiko H, Nakanishi Y. Prognostic evaluation for squamous cell carcinomas of the lower thoracic esophagus treated with three-field lymph node dissection. Eur J Cardiothorac Surg 2001;19:887–93.
30. Hirasaki S, Noguchi T, Mimori K, Onuki J, Morita K, Inoue H, Sugihara K, Mori M, Hirano T. BAC clones related to prognosis in patients with esophageal squamous carcinoma: an array comparative genomic hybridization study. Oncologist 2007;12:406–17.
31. Uchikado Y, Inoue H, Haraguchi N, Mimori K, Natsugoe S, Okumura H, Aikou T, Mori M. Gene expression profiling of lymph node metastasis by oligomicroarray analysis using laser microdissection in esophageal squamous cell carcinoma. Int J Oncol 2006;29:1337–47.
32. Watanabe G, Kaganoi J, Imamura M, Shimada Y, Itami A, Uchida S, Sato F, Kitagawa M. Progression of esophageal carcinoma by loss of EGF-STAT1 pathway. Cancer J 2001;7:132–9.
33. Shimaya K, Shiozaki H, Inoue M, Tahara H, Monden T, Shimano T, Mori T. Significance of p53 expression as a prognostic factor in oesophageal squamous cell carcinoma. Virchows Arch A Pathol Anat Histopathol 1993;422:271–6.
34. Sarbia M, Porschen R, Borchard F, Horstmann O, Willers R, Gabbert HE. p53 protein expression and prognosis in squamous cell carcinoma of the esophagus. Cancer 1994;74:2218–23.
35. Furihata M, Ohtsuki Y, Ogoshi S, Takahashi A, Tamiya T, Ogata T. Prognostic significance of human papillomavirus genomes (type-16, -18) and aberrant expression of p53 protein in human esophageal cancer. Int J Cancer 1993;54:226–30.
36. Wang DY, Xiang YY, Tanaka M, Li XR, Li JL, Shen Q, Sugimura H, Kino I. High prevalence of p53 protein overexpression in patients with esophageal cancer in Linxian. China and its relationship to progression and prognosis. Cancer 1994;74:3089–96.
37. Piessen G, Jonckheere N, Vincent A, Hemon B, Ducourouble MP, Copin MC, Mariette C, Van Seuningen I. Regulation of the human mucin MUC4 by taurodeoxycholic and taurochenodeoxycholic bile acids in oesophageal cancer cells is mediated by hepatocyte nuclear factor 1alpha. Biochem J 2007;402:81–91.
38. Carraway KL, Ramsauer VP, Haq B, Carothers Carraway CA. Cell signaling through membrane mucins. Bioessays 2003;25:66–71.
39. Singh AP, Moniaux N, Chauhan SC, Meza JL, Batra SK. Inhibition of MUC4 expression suppresses pancreatic tumor cell growth and metastasis. Cancer Res 2004;64:622–30.
40. Fauquette V, Perrais M, Cerulis S, Jonckheere N, Ducourouble MP, Aubert JP, Pigny P, Van Seuningen I. The antagonistic regulation of human MUC4 and ErbB-2 genes by the Ets protein PEA3 in pancreatic cancer cells: implications for the proliferation/differentiation balance in the cells. Biochem J 2005;386:35–45.
41. Mendez E, Fan W, Choi P, Agoff SN, Whipple M, Farwell DG, Futran ND, Weymuller EA, Jr, Zhao LP, Chen C. Tumor-specific genetic expression profile of metastatic oral squamous cell carcinoma. Head Neck 2007;29:803–14.
42. Pennathur A, Luketich JD. Resection for esophageal cancer: strategies for optimal management. Ann Thorac Surg 2008;85:S751–6.
43. Kalinin AE, Kajava AV, Steinert PM. Epithelial barrier function: assembly and structural features of the cornified cell envelope. Bioessays 2002;24:789–800.
44. Kim IG, Gorman JJ, Park SC, Chung SI, Steinert PM. The deduced sequence of the novel protransglutaminase E (TGase3) of human and mouse. J Biol Chem 1993;268:12682–90.
45. Chen BS, Wang MR, Xu X, Cai Y, Xu ZX, Han YL, Wu M. Transglutaminase-3, an esophageal cancer-related gene. Int J Cancer 2000; 88:862–5.
46. Luo A, Kong J, Hu G, Liew CC, Xiong M, Wang X, Ji J, Wang T, Zhi H, Wu M, Liu Z. Discovery of Ca2+-relevant and differentiation-associated genes downregulated in esophageal squamous cell carcinoma using cDNA microarray. Oncogene 2004;23:1291–9.